

1 Interferences on Aerosol Acidity Quantification due to Gas-phase Ammonia Uptake onto

2 Acidic Sulfate Filter Samples

3 Benjamin A. Nault^{1,2,*}, Pedro Campuzano-Jost^{1,2}, Douglas A. Day^{1,2}, Hongyu Guo^{1,2}, Duseong S.
4 Jo^{1,2,**}, Anne V. Handschy^{1,2}, Demetrios Pagonis^{1,2}, Jason C. Schroder^{1,2,***}, Melinda K.
5 Schueneman^{1,2}, Michael J. Cubison³, Jack E. Dibb⁴, Alma Hodzic⁵, Weiwei Hu⁶, Brett B. Palm⁷,
6 Jose L. Jimenez^{1,2}

7

8 1. Department of Chemistry, University of of Colorado, Boulder, CO, USA

9 2. Cooperative Institute for Research in Environmental Sciences, University of Colorado,
10 Boulder, CO, USA

11 3. TOFWERK AG, Boulder, CO USA

12 4. Earth Systems Research Center, Institute for the Study of Earth, Oceans, and Space,
13 University of New Hampshire, Durham, NH, USA

14 5. Atmospheric Chemistry Observations and Modeling Laboratory, National Center for
15 Atmospheric Research, Boulder, CO, USA

16 6. State Key Laboratory at Organic Geochemistry, Guangzhou, Institute of Geochemistry,
17 Chinese Academy of Sciences, Guangzhou, China

18 7. Department of Atmospheric Sciences, University of Washington, Seattle, WA, USA

19 * Now at: Center for Aerosols and Cloud Chemistry, Aerodyne Research, Inc., Billerica, MA,
20 USA

21 ** Now at: Advanced Study Program, National Center for Atmospheric Research, Boulder, CO
22 USA

23 *** Now at: Colorado Department of Public Health and Environment, Denver, CO, USA

24

25 Correspondence: Jose L. Jimenez (jose.jimenez@colorado.edu)

26 Abstract

27 Measurements of the mass concentration and chemical speciation of aerosols are important to
28 investigate their chemical and physical processing from near emission sources to the most
29 remote regions of the atmosphere. A common method to analyze aerosols is to collect them onto
30 filters and to analyze filters off-line; however, biases in some chemical components are possible
31 due to changes in the accumulated particles during the handling of the samples. Any biases
32 would impact the measured chemical composition, which in turn affects our understanding of
33 numerous physico-chemical processes and aerosol radiative properties. We show, using filters
34 collected onboard the NASA DC-8 and NSF C-130 during six different aircraft campaigns, a
35 consistent, substantial difference in ammonium mass concentration and ammonium-to-anion
36 ratios, when comparing the aerosols collected on filters versus the Aerodyne Aerosol Mass
37 Spectrometer (AMS). Another *on-line* measurement is consistent with the AMS in showing that
38 the aerosol has lower ammonium-to-anion ratios than obtained by the filters. Using a gas uptake
39 model with literature values for accommodation coefficients, we show that for ambient ammonia
40 mixing ratios greater than 10 ppbv, the time scale for ammonia reacting with acidic aerosol on
41 filter substrates is less than 30 s (typical filter handling time in the aircraft) for typical aerosol
42 volume distributions. Measurements of gas-phase ammonia inside the cabin of the DC-8 show
43 ammonia mixing ratios of 45 ± 20 ppbv, consistent with mixing ratios observed in other indoor
44 environments. This analysis enables guidelines for filter handling to reduce ammonia uptake.
45 Finally, a more meaningful limit-of-detection for SAGA filters collected during airborne
46 campaigns is $\sim 0.2 \mu\text{g sm}^{-3}$ ammonium, which is substantially higher than the limit-of-detection
47 of the ion chromatography. A similar analysis should be conducted for filters that collect
48 inorganic aerosol and do not have ammonia scrubbers and/or are handled in the presence of
49 human ammonia emissions.

50 **Introduction**

51 Particulate matter (PM), or aerosol, impacts human health, ecosystem health, visibility,
52 climate, cloud formation and lifetime, and atmospheric chemistry (Meskhidze et al., 2003;
53 Abbatt et al., 2006; Seinfeld. and Pandis, 2006; Jimenez et al., 2009; Myhre et al., 2013; Cohen
54 et al., 2017; Hodzic and Duvel, 2018; Heald and Kroll, 2020; Pye et al., 2020). Quantitative
55 measurements of the chemical composition and aerosol mass concentration are necessary to
56 understand these impacts and to constrain and improve chemical transport models (CTMs). The
57 inorganic portion of aerosol, which includes both volatile (e.g., nitrate, ammonium) and
58 non-volatile (e.g., calcium, sodium) species, controls many of these impacts through the
59 regulation of charge balance, aerosol pH, and aerosol liquid water concentration (Guo et al.,
60 2015, 2018; Hennigan et al., 2015; Nguyen et al., 2016; Pye et al., 2020). Further, the inorganic
61 portion of aerosol is an important fraction of the aerosol budget, both in polluted cities (e.g.,
62 Jimenez et al., 2009; Song et al., 2018), and remote regions (e.g., Hodzic et al., 2020), and the
63 chemistry controlling the inorganic portion of the aerosol is still not well known (e.g., Liu et al.,
64 2020).

65 There are numerous methods to quantify the inorganic aerosol composition and mass
66 concentration, including by mass spectrometry (DeCarlo et al., 2006; Canagaratna et al., 2007;
67 Pratt and Prather, 2010; Froyd et al., 2019), *on-line* ion chromatography (Talbot et al., 1997;
68 Weber et al., 2001; Nie et al., 2010), and collection onto filters to be extracted and measured
69 off-line by ion chromatography (Malm et al., 1994; Dibb et al., 2002, 2003; Coury and Dillner,
70 2009; Watson et al., 2009). Each method has different advantages and disadvantages (e.g., time
71 resolution, sample preparation, range of species identified, cost, and personnel needs). These

72 results, in turn, have been used to inform and improve the results of CTMs, influencing our
73 understanding in processes such as the direct radiative effect (Wang et al., 2008b), transport of
74 ammonia in deep convection (Ge et al., 2018), aerosol pH (Pye et al., 2020; Zakoura et al., 2020)
75 and subsequent chemistry, and precursor emissions (Henze et al., 2009; Heald et al., 2012;
76 Walker et al., 2012; Mezuman et al., 2016).

77 Filter measurements have been shown to be most prone to artifacts during sample
78 collection, handling, storage of the filter, or extraction of the aerosol from the filter prior to
79 analysis. These artifacts include evaporation of volatile compounds such as organics (Watson et
80 al., 2009; Chow et al., 2010; Cheng and He, 2015) and ammonium nitrate (Hering and Cass,
81 1999; Chow et al., 2005; Nie et al., 2010; Liu et al., 2014, 2015; Heim et al., 2020), as well as
82 chemical reactions of gas-phase species with the accumulated particles (e.g., Schauer et al.,
83 2003; Dzepina et al., 2007). Further, early research indicated potential artifacts from gas-phase
84 ammonia uptake onto acidic aerosol collected onto filters, leading to a positive bias for
85 particulate ammonium (Klockow et al., 1979; Hayes et al., 1980; Koutrakis et al., 1988). This led
86 to debates about whether aerosol in the lower stratosphere was sulfuric acid or ammonium
87 sulfate (Hayes et al., 1980); however, after improved filter handling practices and *on-line*
88 measurements (i.e., mass spectrometry), it has been generally well accepted that the sulfate in the
89 stratosphere is mainly sulfuric acid (Murphy et al., 2014).

90 This artifact may impact aerosols collected in remote locations (e.g., the lower
91 stratosphere, but also the free troposphere over the Pacific Ocean basin). Comparisons for a
92 major cation, ammonium, in a similar location (middle of the Pacific Ocean) have shown very
93 different results (Dibb et al., 2003; Paulot et al., 2015). This, in turn, affects the observed charge

94 balance of anions (sulfate and nitrate) with ammonium, which can indicate different aerosol
95 phase state (Colberg et al., 2003; Wang et al., 2008a) and aerosol pH (Pye et al., 2020), leading
96 to potentially important chemical and physical differences between the real state of the particles
97 and that concluded from the measurements. An example of the differences in observed charge
98 balance of ammonium to sulfate for different studies of the same remote Pacific Ocean region is
99 highlighted in Fig. 1. This difference leads to the inorganic portion of the aerosol potentially
100 being solid (filters) and hence good ice-nucleating particles (Abbatt et al., 2006), versus it being
101 liquid (*on-line* measurements), leading to important differences in the calculated radiative
102 balance. It should be noted that other measurements (both filter and *on-line*) in a similar location
103 from another study (bar at surface (Paulot et al., 2015)) are more in-line with the *on-line*
104 observations. A large decrease in the ambient ammonia mixing ratio is required to change from
105 ammonium sulfate-like aerosols to sulfuric acid-like aerosols between the years, contradictory to
106 the increasing trends of ammonia globally (Warner et al., 2016, 2017; Weber et al., 2016; Liu et
107 al., 2019; Tao and Murphy, 2019). Further, oceanic emissions of ammonia are not high enough to
108 lead to full charge neutralization of sulfate, since these emissions are approximately an order of
109 magnitude less than those of sulfate precursors (Faloona, 2009; Paulot et al., 2015). A debate
110 about the acidity and potential impact of ammonia-uptake artifacts on acidic filters for remote
111 locations has not occurred as it did for stratospheric observations.

112 Previous laboratory studies have suggested that exposure of acidic aerosol, both
113 suspended in air in a flow tube or on a filter, to gas-phase ammonia will lead to formation of
114 ammonium salts in short time (≤ 10 s) (Klockow et al., 1979; Huntzicker et al., 1980); however,
115 it has not been investigated if this time frame applies for acidic aerosol collected on filters

116 handled in a typical indoor environment. Though human emissions of ammonia are variable and
117 depend on various factors (e.g., temperature, clothing, etc.) (Li et al., 2020), the emissions of
118 ammonia, specifically from perspiration but also from breath, can lead to high, accumulated
119 mixing ratios of ammonia indoor (e.g., Ampollini et al., 2019; Finewax et al., 2020) and
120 references therein), depending on the ventilation rate. The mixing ratios of ammonia can be
121 factor of 2 to 2000 higher indoor versus outdoor. This higher mixing ratio of ammonia leads to
122 similarly high mixing ratios used in prior studies to lead to partially to fully neutralize sulfuric
123 acid (Klockow et al., 1979; Huntzicker et al., 1980; Daumer et al., 1992; Liggio et al., 2011).

124 Here, we investigate whether previously observed laboratory observations of ammonium
125 uptake to acidic particulate lead to the large differences in ammonium, both in mass
126 concentration and in ammonium-to-sulfate ratios or ammonium-to-anion ratios, between *in-situ*
127 measurements and *off-line* filter measurement during five NASA and one NSF airborne
128 campaigns that sampled air over remote continental and oceanic regions. An uptake model for
129 gas-phase ammonia interacting with acidic PM on a filter along with constraints from
130 observations of gas-phase ammonia in the cabin of the airplane are used to further probe the
131 reason behind the differences between the *in-situ* and *off-line* measurements of ammonium. The
132 results provide insight into how to interpret prior aircraft measurements and other filter based
133 measurements where the filters were handled in environments (i.e., indoors), where rapid uptake
134 of ammonia to acidic PM will occur.

135

136 **2. Methods**

137 **2.1 Aircraft Campaigns**

138 Five different NASA aircraft campaigns on-board the DC-8 research aircraft and one
139 NSF aircraft campaign on-board the C-130 research aircraft are used in this study. As described
140 below, though the campaigns were sampling ambient (outside) air in various locations around the
141 world, the filters were handled and exposed to both aircraft cabin air and indoor temporary
142 laboratory air, where between 20 and 40 people were operating instruments. The campaigns
143 include the Arctic Research of the Composition of the Troposphere from Aircraft and Satellites
144 (ARCTAS) -A (April 2008) and -B (June – July 2008) campaigns (Jacob et al., 2010), the
145 Studies of Emissions and Atmospheric Composition, Clouds, and Climate Coupling by Regional
146 Surveys (SEAC⁴RS, August – September 2013) campaign (Toon et al., 2016), the Wintertime
147 INvestigation of Transport, Emissions, and Reactivity (WINTER, February – March 2015)
148 (Schroder et al., 2018), and the Atmospheric Tomography (ATom) -1 (July – August 2016) and
149 -2 (January – February 2017) campaigns (Hodzic et al., 2020). ARCTAS-A was based in
150 Fairbanks, Alaska, Thule, Greenland, and Iqaluit, Nunavut, and sampled the Arctic Ocean and
151 Arctic regions of Alaska, Canada, and Greenland; while, ARCTAS-B was based in Cold Lake,
152 Alberta, Canada, and sampled the boreal Canadian forest, including wildfire smoke. SEAC⁴RS
153 was based in Houston, Texas, and sampled biomass burning from western forest fires and
154 agricultural burns along the Mississippi River and the Southern United States, isoprene
155 chemistry over Southern United States and midwestern deciduous forests, and deep convection
156 associated with isolated thunderstorms, the North American Monsoon, and tropical depressions.
157 Finally, ATom-1 and -2 sampled the remote atmosphere over the Arctic, Pacific, Southern, and
158 Atlantic Oceans during the Northern (Southern) Hemispheric summer (winter) and winter
159 (summer).

160 For ARCTAS-A, -B, and SEAC⁴RS, the general sampling scheme was regional, sampling
161 large regions at level flight tracks. ATom-1 and -2, being global in nature, only sampled at level
162 legs for short durations (5 – 15 min) at low (~300 m) and high (10 – 12 km) altitude, and did not
163 measure at level altitudes between the low and high altitude. Due to the sampling time of the
164 filters (see Sect. 2.2.2), the entirety of the ascent and descent time was needed for one filter
165 sample. Therefore, all data during the ascents and descents have not been considered in this
166 study to minimize any issues due to the mixing of aerosols of different compositions and
167 acidities.

168

169 **2.2 Aerosol Measurements**

170 **2.2.1 Aerosol Mass Spectrometer**

171 An Aerodyne High-Resolution Time-of-Flight Aerosol Mass Spectrometer, flown by the
172 University of Colorado-Boulder (CU for short), was flown during the five campaigns used here.
173 The general features of the AMS have been described in prior studies (DeCarlo et al., 2006;
174 Canagaratna et al., 2007), and the specifics of the CU AMS for each campaign has been
175 described elsewhere (Cubison et al., 2011; Liu et al., 2017; Nault et al., 2018; Schroder et al.,
176 2018; Guo et al., 2020; Hodzic et al., 2020). In brief, the AMS measured the mass concentration
177 of non-refractory species in PM₁ (PM with an aerodynamic diameter less than 1 μm, see Guo et
178 al. (2020) for details). Ambient air was sampled by drawing air through an NCAR
179 High-Performance Instrumental Platform for Environmental Modular Inlet (HIMIL; Stith et al.
180 (2009)) at a constant standard flow rate of 9 L min⁻¹ (T = 273.15 K and P = 1013 hPa). The best
181 estimated upper size cut-off for the HIMIL inlet is ~1 μm diameter (geometric, David Rogers,

182 pers. comm. 2011). This diameter is larger than the size cut-off than that of the AMS inlet
183 (~0.5-0.7 μm diameter, geometric, depending on the composition), with no losses in the tubing
184 between the HIMIL and AMS inlet expected (see Guo et al. (2020) for more details). Multiple
185 comparisons with instruments sampling from an isokinetic inlet PM_4 inlet (Brock et al., 2019;
186 Guo et al., 2020) indicate that no significant sampling biases were incurred over the size range of
187 the AMS. No active drying of the sampling flow was used to minimize artifacts for semi-volatile
188 species, but the temperature differential between ambient and cabin typically ensured the relative
189 humidity (RH) inside the sampling line less than 40% (e.g., Nault et al., 2018). An exception to
190 this was during ATom-1 and -2, where the cabin temperature, along with the high RH in tropics,
191 led to higher RH in the sample lines in a few instances in the boundary layer, which was
192 accounted for in the final mass concentrations (Guo et al., 2020). To minimize any potential
193 losses of volatile aerosol components, the residence time between the inlet and AMS was less
194 than 1 s (Nault et al., 2018; Schroder et al., 2018; Guo et al., 2020). Prior studies (Guo et al.,
195 2016; Shingler et al., 2016) have shown minimal loss of semivolatile components for this
196 residence time.

197 The air sample was introduced into the AMS via an aerodynamic focusing lens (Zhang et
198 al., 2002, 2004), which was operated at 2.00 hPa (1.50 Torr), via a pressure-controlled inlet,
199 which was operated at various pressures (94-325 Torr) (Bahreini et al., 2008), depending on the
200 ceiling of the campaign and lens transmission calibrations (Hu et al., 2017b; Nault et al., 2018).
201 The aerosol, once focused, was introduced into a detection chamber after three differential
202 pumping stages. The aerosol impacted on an inverted cone porous tungsten “standard” vaporizer
203 under high vacuum, which was held at $\sim 600^\circ\text{C}$. Upon impaction, the non-refractory portion of

204 the aerosol (organic, ammonium, nitrate, sulfate, and chloride) were flash-vaporized, and the
205 vapors were ionized by 70 eV electron ionization. The ions were then extracted and analyzed
206 with a H-TOF time-of-flight mass spectrometer (Tofwerk AG). The AMS was operated in the
207 “V-mode” ion path (DeCarlo et al., 2006), with spectral resolution ($m/\Delta m$) of 2500 at m/z 44 and
208 2800 at m/z 184. The collection efficiency (CE) for AMS was estimated with the
209 parameterization of Middlebrook et al. (2012), which has been shown to perform well for
210 ambient aerosols (Hu et al., 2017a, 2020). The AMS nominally samples aerosol with vacuum
211 aerodynamic diameter between 40 nm and 1400 nm, which was calibrated for in SEAC⁴RS,
212 ATom-1, and -2 (Liu et al., 2017; Guo et al., 2020). Mass and/or volumen closure has been
213 investigated between the AMS and other measurements for all campaigns discussed here
214 (Cubison et al., 2011; Aknan, 2015; Liu et al., 2017; Nault et al., 2018; Schroder et al., 2018;
215 Guo et al., 2020). The closure was complete for the size range of the AMS and did not show any
216 dependence with altitude (Guo et al., 2020). Software packages Squirrel and PIKA under Igor
217 Pro 7 (WaveMetrics, Lake Oswego, OR) (DeCarlo et al., 2006; Sueper, 2018) were used to
218 analyze all AMS data.

219 A cryogenic pump, to reduce background of ammonium and organics (Nault et al., 2018;
220 Schroder et al., 2018), was flown on the AMS for SEAC⁴RS, ATom-1, and -2; but not for
221 ARCTAS-A and -B. The cryogenic pump lowers the temperature of a copper cylinder
222 surrounding the vaporizer to ~90 K. This freezes out the background gases and ensures low
223 detection limits from the beginning of the flight, which is critical since aircraft instruments can
224 typically not be pumped continuously and hence suffer from high backgrounds at switch-on. The

225 2σ accuracy for the AMS for inorganic aerosol is estimated to be 35% (Bahreini et al., 2009; Guo
226 et al., 2020).

227

228 **2.2.2 Aerosol Filters**

229 Fast collection of aerosol particles onto filters during airborne sampling, via the
230 University of New Hampshire Soluble Acidic Gases and Aerosol (SAGA) technique, has been
231 described elsewhere (Dibb et al., 2002, 2003), and was flown during the five campaigns
232 investigated here. Briefly, air is sampled into the airplane via a curved leading edge nozzle (Dibb
233 et al., 2002). The inlet is operated isokinetically during flight, and typically has a 50% collection
234 efficiency for aerosol with an aerodynamic diameter of $4.1\ \mu\text{m}$ (Dibb et al., 2002; McNaughton
235 et al., 2007), with some altitude dependence (Guo et al., 2020). The lower size cut-offs for
236 SAGA and AMS are similar (Guo et al., 2020). As discussed by Guo et al. (2020; their Fig. 8)
237 the difference in mass sampled at the smaller sizes between SAGA and AMS is generally
238 negligible at all altitudes.

239 Aerosol was collected onto Millipore Fluoropore Teflon filters (90 mm diameter with 1
240 μm pore size). Collection time was dependent on altitude and estimated mass concentration, but
241 generally 2 to 3 sm^3 (where sm^3 is standard m^{-3} at temperature = 273 K and pressure = 1013 hPa)
242 volume of air is collected to ensure detectable masses of species (Dibb et al., 2002). The aerosol
243 inlet flow is close to 400 slpm in the marine boundary layer and approximately 150 slpm at
244 maximum altitude. Further, 2 blank filters are collected each flight. The filters were contained in
245 a Delrin holder during collection. After collection, the filters were transferred to a particle free
246 polyethylene “clean room” bag, which was filled with zero air, sealed, and stored over dry ice.

247 No acid scrubbers were inserted into the bags to prevent any artifact from offgassing of
248 ammonia. The samples from the filters were then extracted during non-flight days with 20 mL
249 ultrapure water and preserved with 100 μ L chloroform (see Sect. S2). The preserved samples
250 were sent to the University of New Hampshire, to be analyzed by ion chromatography. The
251 estimated limit of detection for both sulfate and ammonium is $0.01 \mu\text{g sm}^{-3}$ for all missions
252 evaluated here (Dibb et al., 1999).

253

254 **2.2.3 Other Aerosol Measurements**

255 The NOAA Particle Analysis by Laser Mass Spectrometer (herein PALMS) was flown
256 during ATom-1 and -2. Details of the PALMS instrument configured for ATom-1 and -2 are
257 described in Froyd et al. (2019). Briefly, PALMS measures the chemical composition of single
258 aerosol particles via laser-ablation/ionization (Murphy and Thomson, 1995; Thomson et al.,
259 2000), where the ions are extracted and detected by a time of flight mass spectrometer. The
260 instrument measures particles between 100 nm and $4.8 \mu\text{m}$ (geometric diameter) (Froyd et al.,
261 2019). The measurement of PALMS used in this study is the “sulfate acidity indicator” (Froyd et
262 al., 2009). These authors reported that in the negative ion mode, there is a prominent peak at m/z
263 97, corresponding to HSO_4^- , and another peak at m/z 195, corresponding to the cluster
264 $\text{HSO}_4^-(\text{H}_2\text{SO}_4)$. The first peak was independent of acidity; whereas, the second peak was
265 dependent on acidity. Froyd et al. (2009) calibrated the PALMS ratio of
266 $\text{HSO}_4^-(\text{H}_2\text{SO}_4)/(\text{HSO}_4^-+\text{HSO}_4^-(\text{H}_2\text{SO}_4))$ to Particle-into-Liquid Sampler (PILS) measurements to
267 achieve an estimate of ammonium balance.

268 Besides the chemical composition, the particle number and volume distributions are used
269 here. For SEAC⁴RS, the measurements have been described elsewhere (e.g., Liu et al., 2016).
270 The laser aerosol spectrometer (from TSI), which measured aerosol from geometric diameter 100
271 nm to 6.3 μm , is used here for volume distribution. For the ATom missions, the measurements
272 have been described elsewhere (Kupc et al., 2018; Williamson et al., 2018; Brock et al., 2019).
273 Briefly, the dry particle size distribution, from geometric diameter of 2.7 nm to 4.8 μm , were
274 measured by a series of optical particle spectrometers, including the Nucleation Model Aerosol
275 Size Spectrometer (3 nm to 60 nm, custom built (Williamson et al., 2018)), an Ultra-High
276 Sensitivity Aerosol Spectrometer (60 nm to 1 μm) from Droplet Measurement Technologies
277 (Kupc et al., 2018), and Laser Aerosol Spectrometer (120 nm to 4.8 μm) from TSI. These
278 measurements have been split in nucleation mode (3 to 12 nm), Aitken mode (12 to 60 nm),
279 accumulation mode (60 to 500 nm) and coarse mode (500 nm to 4.8 μm).

280

281 **2.3 Gas-Phase and Other Measurements**

282 **2.3.1 Ammonia Measurements**

283 Gas-phase ammonia was measured inside the cabin of the NASA DC-8 during the
284 FIREX-AQ campaign (Warneke et al., 2018), a subsequent DC-8 campaign which shared many
285 instrument installations and a similar level of aircraft personnel with the campaigns analyzed
286 here. The location of the instrument and where it sampled cabin ammonia (in relation to where
287 the SAGA filters are located) is shown in Fig. S1. Ammonia was measured by a Picarro G2103
288 Gas Concentration Analyzer (von Bobruzki et al., 2010; Sun et al., 2015; Kamp et al., 2019).
289 The instrument is a continuous, cavity ring-down spectrometer. Cabin air is brought into a cavity

290 at low pressure (18.7 kPa, 140 Torr), where laser light is pulsed into the cavity. The light is
291 reflected by mirrors in the cavity, providing an effective path length of kilometers. A portion of
292 the light penetrates the mirrors, reaching the detectors, where the intensity of the light is
293 measured to determine the mixing ratio of ammonia from the time decay of the light intensity via
294 Beer-Lambert Law. The instrument measures the absorption of infrared light from 6548.5 to
295 6549.2 cm^{-1} (Martin et al., 2016). Absorption of gas-phase water is also measured and corrected
296 for. This water vapor measurement is also used to calculate RH inside the cabin of the DC-8
297 (Filges et al., 2018). Data was logged at 1 Hz.

298

299 **2.3.2 Carbon Dioxide and Temperature Measurements**

300 Carbon dioxide inside the cabin of the NASA DC-8 during FIREX-AQ was measured by
301 a HOBO MX1102 Carbon Dioxide Data Logger (HOBO by Onset). It is a self-calibrating carbon
302 dioxide sensor with a range of 0 to 5,000 ppm carbon dioxide and an accuracy of ± 50 ppm. A
303 non-dispersive infrared sensor is used to measure carbon dioxide. Data was acquired once every
304 10 s to once every 2 min. Besides carbon dioxide, RH and temperature are also recorded by the
305 instrument. Prior to each flight, the instrument was turned on and measured ambient carbon
306 dioxide, outside the cabin of the DC-8, to ensure the accuracy of the instrument compared to
307 ambient carbon dioxide measurements.

308 Ambient carbon dioxide during FIREX-AQ was measured by an updated version of the
309 instrument known as Atmospheric Vertical Observations of CO_2 in the Earth's Troposphere
310 (AVOCET) (Vay et al., 2003, 2011). The updated instrument used a modified LI-COR model
311 7000 non-dispersive infrared spectrometer and measured carbon dioxide at 5 Hz.

312 Temperature in the cabin was measured by a thermocouple (SEAC⁴RS) or thermistor
313 (ATom-1 and 2) located in the AMS rack or a Vaisala probe located at the front of the airplane
314 (ARCTAS-A, -B, and SEAC⁴RS).

315

316 **2.4 Theoretical Ammonia Flux Model**

317 To investigate the possibility that the ammonia mixing ratio in the cabin of the DC-8 is
318 high enough to be taken up by acidic PM on a filter during the short time the filter is exposed to
319 cabin air prior to final storage, a theoretical uptake model was constructed to estimate the time
320 scale for ammonia to interact with all the acidic particles (Seinfeld. and Pandis, 2006). The
321 equations used for the model can be found in the Supplemental Information (Sect. S3). The
322 model was initialized with a range of ammonia mixing ratios (1 to 200 ppb) and a range of PM
323 diameters (10 to 1000 nm). The calculations were conducted at 298 K, which is within ± 10 K of
324 typical temperatures inside the cabin of the NASA DC-8 during the five campaigns (Fig. S2). An
325 accommodation coefficient of 1 for ammonia onto acidic PM was assumed (Hanson and
326 Kosciuch, 2003), with a density of 1.8 g cm^{-3} for sulfuric acid (Rumble, 2019). For the mass
327 transfer calculations, the transition regime (between the free molecular and continuum regimes)
328 equations were used, using the Fuchs and Sutugin parameterization (Fuchs and Sutugin, 1971).
329 The model was used to estimate the ammonia molecular flux to acidic PM on the filter (Eq. S3).
330 Finally, the molecular flux was used to estimate the time it would take all the particles to be
331 partially neutralized by ammonia in the cabin (Eq. S4), though this may be a lower limit
332 (Robbins and Cadle, 1958; Daumer et al., 1992).

333

334 3. Results and Discussion

335 3.1 Comparison of On-Line and Off-Line Ion Balances across the Tropospheric Column

336 SAGA and AMS co-sampled aerosols during multiple aircraft campaigns. Nitrate quickly
337 evaporates from aerosols as the aerosols are transported away from source regions and is
338 typically small in the global troposphere (DeCarlo et al., 2008; Hennigan et al., 2008; Hodzic et
339 al., 2020). Thus, in Fig. 2 the mass concentrations for the two most important submicron
340 contributors to ammonium balance, ammonium and sulfate, are compared from the aircraft
341 campaigns. The campaigns generally sampled remote air, either continental or oceanic, except
342 for biomass burning sampled during ARCTAS-B and SEAC⁴RS and downwind of urban areas
343 during WINTER. The measurements, for mass concentrations greater than $0.1 \mu\text{g sm}^{-3}$, are
344 generally within the combined uncertainties of the two instruments. Sulfate generally remains on
345 the one-to-one line, even at low mass concentrations. However, ammonium shows a large
346 divergence between the two measurements for mass concentrations less than $0.1 \mu\text{g sm}^{-3}$ during
347 all six aircraft campaigns. As shown in Fig. 2, the divergence in ammonium occurs well above
348 the limit-of-detection for both instruments, namely $\sim 4 \text{ ng sm}^{-3}$ for AMS for a 5-minute average
349 (DeCarlo et al., 2006; Guo et al., 2020) and 10 ng sm^{-3} for SAGA (Dibb et al., 1999), for both
350 ammonium and sulfate.

351 This divergence in ammonium mass concentration is thus reflected in the ammonium
352 balance, defined as the ratio of ammonium to sulfate plus nitrate, in moles (Fig. 3). For all
353 campaigns, the two measurements show differences in ammonium balance, especially at higher
354 altitudes, where the aerosols is distant from ammonia emissions (Dentener and Crutzen, 1994;
355 Paulot et al., 2015), but sulfate production can continue due to vertical transport of precursors

356 such as SO₂. On average, the SAGA measurements indicate ammonium balance rarely below 0.5
357 throughout the troposphere; whereas, the AMS measurements indicate that ammonium balance
358 generally drops to below 0.2 for pressures less than 400 hPa. Fig. 2 and Fig. 3 indicate either
359 differences in the ammonium balance due to differences in aerosols population sampled, as
360 SAGA measures larger aerosols diameters than AMS (Guo et al., 2020), or potential artifacts
361 with one of the measurements.

362 Both the AMS and the filters sample most of the submicron aerosols (see Guo et al.
363 (2020) for details), but the filters also sample supermicron particles that the AMS does not.
364 Therefore it is possible in principle that the difference could be due to ammonium present in
365 supermicron particles. As discussed in Guo et al. (2020), nearly 100% of the measured volume
366 occurs for aerosols < 1 μm above the marine boundary layer, where the largest difference in
367 ammonium balance between the filters and AMS occurs (Fig. 3). Further, ammonium has been
368 observed to be a small fraction of the supermicron mass (Kline et al., 2004; Cozic et al., 2008;
369 Pratt and Prather, 2010), except for instances of continental fog (Yao and Zhang, 2012) and
370 Asian dust events (Heim et al., 2020). An upper estimate of supermicron ammonium can be
371 calculated using results from prior studies (Kline et al., 2004; Cozic et al., 2008). In these prior
372 studies, ~90% of the ammonium was submicron. With the average ammonium observed during
373 ATom-1 and -2 (~10 to 50 ng sm⁻³) (Hodzic et al., 2020), that would suggest an upper limit of ~1
374 to 5 ng sm⁻³ ammonium in the supermicron aerosols. This upper estimate does not explain the
375 differences between AMS and filters during ATom-1 and -2 (Fig. S3), as the percent difference
376 increases with decreasing estimated supermicron ammonium volume. As the largest differences
377 between the AMS and filters occur well above the boundary layer (Fig. 3), away from

378 continental ammonia sources (Dentener and Crutzen, 1994) and Asian dust events, we conclude
379 that the sampling of supermicron aerosols by filters is not leading to the observed differences in
380 ammonium.

381 The only useful comparison, other than SAGA versus AMS, is with PALMS during
382 ATom. Prior studies by PALMS have shown aerosols observed for pressure < 400 hPa to be
383 acidic, depending on potential recent influence of boundary layer air via convection (Froyd et al.,
384 2009; Liao et al., 2015), similar to observations by other single particle mass spectrometers (Pratt
385 and Prather, 2010). Though not reaching similarly low $\text{NH}_4/(2\times\text{SO}_4)$ values as the AMS, the
386 PALMS acidity marker shows much lower values than were determined by the aerosols collected
387 on the filters (Fig. S4). Different reasons for PALMS not achieving as low values as AMS may
388 include differences in aerosols sizes sampled by PALMS versus AMS (Guo et al., 2020), and the
389 sensitivity of the acidity marker to laser power (Liao et al., 2015). Thus, two different *on-line*
390 measurements indicate that the ammonium balance is lower than the aerosols collected on filters,
391 suggesting potentially more acidic aerosols.

392 Differences in ammonium balance between AMS and SAGA are detectable for sulfate
393 mass concentrations $\leq 1 \mu\text{g sm}^{-3}$ (Fig. 4) for all six aircraft campaigns. As the sulfate mass
394 concentration decreases, the relative differences in ammonium, and thus ammonium balance,
395 increase. The large majority of the troposphere contains sulfate mass concentrations in which the
396 differences in ammonium are observed, highlighting the importance of this problem (Fig. 4a).
397 Thus, except for more polluted conditions ($> 1 \mu\text{g sm}^{-3}$ sulfate), which mainly occurs in
398 continental (Jimenez et al., 2009; Kim et al., 2015; Malm et al., 2017) and urban regions
399 (Jimenez et al., 2009; Hu et al., 2016; Kim et al., 2018; Nault et al., 2018), this bias between

400 filters and *on-line* measurements is critically important, especially since airborne measurements
401 are often the only meaningful observational constraints for remote regions. Thus, this analysis
402 suggests that for SAGA filters, a more meaningful ammonium limit-of-detection would be
403 equivalent to $1 \mu\text{g sm}^{-3}$ sulfate, which would be $\sim 0.2 \mu\text{g sm}^{-3}$ ammonium. This also provides the
404 framework to define limit-of-detection for other filter-based measurements not associated with
405 ion chromatography.

406

407 **3.2 Ammonia Levels on the NASA DC-8 Cabins**

408 Prior studies have suggested that various sources of ammonia could impact acidic filter
409 measurements (Klockow et al., 1979; Hayes et al., 1980; Koutrakis et al., 1988). Some of these
410 studies found that the materials of the containers where the filters are stored, unless thoroughly
411 cleaned and not stored around humans, are a source of ammonia gas that reacts with the sulfuric
412 acid on the filters to become ammonium, leading to ammonium bisulfate or ammonium sulfate
413 (Hayes et al., 1980). Further, handling of acidic filters in rooms with people or acidic aerosol in
414 the presence of human breath can also lead to near to complete neutralization of acidic aerosol
415 (Larson et al., 1977; Hayes et al., 1980; Clark et al., 1995). Finally, various studies have
416 suggested that the SAGA filters specifically may be impacted by various ammonia sources prior
417 to sampling with the ion chromatography (Dibb et al., 1999, 2000; Fisher et al., 2011).

418 During SAGA sampling, the filters with collected aerosol are moved from the sample
419 collector to a polyethylene bag that is filled with clean air. During this step, the filter is exposed
420 to the cabin air of the DC-8 for ~ 10 s. As humans are a source of ammonia (Larson et al., 1977;
421 Clark et al., 1995; Sutton et al., 2000; Finewax et al., 2020; Li et al., 2020), this source sustains

422 significant ammonia concentrations in indoor environments, which could potentially bias the
423 filter measurements. *On-line* measurements would not be subject to this effect since the sampled
424 air is not exposed to cabin air before measurement. While inlet lines for *on-line* instruments
425 could in theory lead to some memory effects, there is no evidence of such effects in the data
426 (e.g., the response going from a large, neutralized plume into the acidic FT is nearly
427 instantaneous (Schroder et al., 2018)).

428 During a recent 2019 NASA DC-8 aircraft campaign, FIREX-AQ, ammonia was
429 measured on-board the DC-8 during several research flights. An example time series of cabin
430 ammonia, temperature, and RH is shown in Fig. 5. Prior to take-off, as scientists were slowly
431 boarding the airplane, the ammonia mixing ratio was low (< 20 ppbv) and similar to ambient
432 levels of ammonia outside the aircraft. As scientists started boarding before take-off, the
433 ammonia mixing ratio increased. Upon doors closing, the mixing ratio leveled off at ~ 40 ppbv.
434 After take-off, the mixing ratio remained ~ 40 ppbv, though there were changes related to
435 changes in cabin temperature and humidity, which would affect emission rates and also
436 adsorption of ammonia onto cabin surfaces (Sutton et al., 2000; Finewax et al., 2020; Li et al.,
437 2020) and movement of scientists throughout the cabin, which would affect emission rates and
438 their location.

439 The average ($\pm 1\sigma$ spread of the observations) and median ammonia in the cabin of the
440 DC-8 during FIREX-AQ was 45.4 ± 19.9 and 41.9 ppbv (Fig. 6). There was a large positive tail in
441 ammonia mixing ratio, related to high temperatures (Fig. S5), which causes the scientists to
442 perspire more and release more ammonia (Sutton et al., 2000; Finewax et al., 2020; Li et al.,
443 2020). Compared to outdoor ammonia mixing ratios, ranging from urban to remote locations, the

444 ammonia in the cabin of the DC-8 is higher by a factor of 2 to 2000 (Fig. 6). On the other hand,
445 the ammonia measured in the cabin of the DC-8 is similar but towards the lower end of the
446 mixing ratios measured during various indoor studies (Table S1 for compilation of references).

447 The ammonia mixing ratios observed in the cabin were verified by investigating the cabin
448 air exchange rates (see SI Sect. S3). Using carbon dioxide measurements, the exchange rate in
449 the cabin was calculated to be 9.9 hr^{-1} (Fig. S6), which is similar to literature values for the cabin
450 exchange rate of other passenger airliners (Hunt and Space, 1994; Hocking, 1998; Brundrett,
451 2001; National Research Council, 2002). This value is a factor of 2 to 5 higher than typical
452 exchange rates for commercial buildings (Hunt and Space, 1994; Pagonis et al., 2019), which
453 would suggest lower mixing ratios than observed in other indoor environments. Using this
454 exchange rate, and the literature total ammonia emission rates from humans ($1940 \mu\text{g hr}^{-1}$
455 person^{-1} (Sutton et al., 2000)) and the average of ambient ammonia mixing ratios as an outdoor
456 background onto which the human emissions in the cabin are added ($\sim 4.4 \text{ ppbv}$, Fig. 6), the
457 ammonia mixing ratio in the cabin of the DC-8 was estimated to be 43.4 ppbv , which is within
458 the uncertainty of the average ammonia ($45.4 \pm 19.9 \text{ ppbv}$) inside the cabin of the DC-8. Thus, the
459 observed ammonia mixing ratios in the cabin of the DC-8 are consistent with the cabin air
460 exchange rates and literature human ammonia emissions. These mixing ratios are approximately
461 a factor of nine higher than in a typical laboratory environment (Fig. S7), as there are fewer
462 people (1 to 4 versus 20 to 40), making the cabin of the DC-8 an extreme laboratory environment
463 for handling acidic filters. As shown in Fig. 6, ammonia mixing ratios in indoor environments
464 are high enough to change the thermodynamics of inorganic aerosol, leading to higher
465 ammonium balances (Weber et al., 2016). Thus, similar to the conclusions of other studies, the

466 cabin of the DC-8 is an important source of ammonia that could lead to biases with acidic
467 aerosols collected on filters.

468 During FIREX-AQ, the DC-8 frequently sampled air impacted by biomass burning,
469 which is an important source of ammonia (Sutton et al., 2013) and could potentially increase the
470 background ammonia being brought into and mixing with the cabin air being sampled by the
471 Picarro. Splitting the cabin ammonia ratios between sampling air impacted by biomass burning
472 versus nominally background air, the normalized PDF did not shift to higher ammonia mixing
473 ratios (Fig. S7). Further, the averages of the observed cabin ammonia was statistically similar, at
474 the 95% confidence interval, between the DC-8 sampling biomass burning and nominally
475 background air (48.1 ± 13.4 versus 44.1 ± 14.4 ppbv for biomass burning and background air,
476 respectively). Finally, the majority of the time the cabin air was sampled by the Picarro for cabin
477 ammonia, the DC-8 was sampling agricultural fires in Southeast US, which are shorter in
478 duration (seconds) versus the large wildfires in Western US (minutes to hours). This is reflected
479 in the low average ambient value for ammonia, as measured by a proton transfer reaction mass
480 spectrometer (Müller et al., 2014), when the DC-8 was sampling biomass burning-influenced air
481 observed during this time (~ 10 ppbv) and very low average value for non-biomass
482 burning-influenced air (~ 0.8 ppbv) (Fig. S7). Thus, ammonia from biomass burning would at
483 most be a small impact on the ammonia measured in the cabin of the DC-8, further indicating the
484 ammonia in the cabin was mainly from human emissions.

485

486 **3.3 Can Uptake of Cabin Ammonia Explain the Higher Ammonium Concentrations on**
487 **Filters?**

488 As shown in Fig. 6, the cabin of the DC-8 is an important source of ammonia from the
489 breathing and perspiring of scientists. Prior studies (Klockow et al., 1979; Huntzicker et al.,
490 1980; Daumer et al., 1992; Liggio et al., 2011) have shown in laboratory settings that 10 s is fast
491 enough to partially to fully neutralize sulfuric acid. Thus, here we investigate whether the time of
492 the filter handling of 10 s will lead to partial to full neutralization of sulfuric acid from cabin
493 ammonia, or whether this time is fast enough to limit exposure of the acidic filter to cabin
494 ammonia. Huntzicker et al. (1980) showed that for typical aerosol modal distributions (Fig. 7)
495 and cabin RH (Fig. S9), an initial pure sulfuric acid aerosol, suspended in a flow reactor, reaches
496 equal molar amounts of ammonium and sulfate (i.e., ammonium bisulfate) when exposed to 70
497 ppb ammonia in 10 s. This indicates the plausibility that acidic aerosol filters, which typically
498 have lower sulfate mass concentrations than Huntzicker et al. (1980) ($\sim 2 \mu\text{g}$ versus $\sim 55 \mu\text{g}$
499 sulfate equivalent on filters), would interact with cabin ammonia to form at least ammonium
500 bisulfate. Further, other studies found that in less than 10 s, sulfuric acid aerosol, suspended in a
501 flow reactor, at $\text{RH} \leq 45\%$, will completely react with gas-phase ammonia to form ammonium
502 sulfate (Robbins and Cadle, 1958; Daumer et al., 1992). The latter study used ammonia mixing
503 ratios similar to the amount observed in the cabin of the DC-8 ($\sim 30 \text{ ppbv}$); whereas, the former
504 study used excess ammonia ($\sim 9 \text{ ppmv}$). Some studies have suggested that the bags used to store
505 the filters may be a source of ammonia (e.g., Hayes et al., 1980); however, calculations indicate
506 the bags would be a small source of ammonia (see Sect. S4).

507 First, the time of diffusion of ammonia gas from the surface to the interior of the filter
508 was investigated, as there is a potential for the PM to be embedded deep into the filter. Eq. 1
509 (Seinfeld. and Pandis, 2006):

510
$$\tau_{diffusion} = \frac{d_t^2}{8D_g}$$
 Eq. 1

511 where d_t^2 is the depth of the Teflon (~0.015 cm) and D_g is the diffusion coefficient of ammonia in
512 air ($0.228 \text{ cm}^2 \text{ s}^{-1}$) (Spiller, 1989). Therefore, the estimated timescale for ammonia to diffuse
513 through the depth of the Teflon filter is $\sim 1 \times 10^{-4}$ s, meaning that the surface of PM will always be
514 in contact with cabin-level mixing ratios of ammonia. Even though the filters have a porous
515 membrane, for molecular diffusion, the membrane only increases the pathway that the ammonia
516 molecules have to travel slightly; thus, not changing the estimated time. Second, as the particles
517 are liquid (Wilson, 1921), the diffusion will be similar as through water. A typical value for
518 diffusivity in water is $\sim 1 \times 10^{-5} \text{ cm}^2 \text{ s}^{-1}$ (Seinfeld. and Pandis, 2006). For the size ranges observed
519 (Fig. 7, ~40 - 700 nm), this corresponds to a timescale of 1.6×10^{-7} to 5.0×10^{-5} s. Thus, the
520 diffusion through the filter and through the PM is nearly instantaneous for ammonia.

521 A theoretical uptake model for ammonia to acidic PM on filters was run for a range of
522 ammonia mixing ratios and PM diameters (Fig. 7). As shown in Fig. 7, only at the lowest
523 ammonia mixing ratios (< 10 ppbv), the flux of ammonia to acidic PM is slower (> 20 s) than the
524 typical filter handling time (~10 s) for typical aerosol diameters in the remote atmosphere. For
525 the conditions of the DC-8, similar to other indoor environments (> 20 ppbv ammonia, Fig. 6),
526 and ambient aerosol diameters in the accumulation mode that contains most ambient sulfate
527 (Fig. 7), the amount of time needed for cabin ammonia to interact with acidic PM on filters to
528 form ammonium bisulfate is ≤ 10 s, similar to the results of Huntzicker et al. (1980). Also,
529 studies show that the kinetic limitation to form ammonium sulfate $((\text{NH}_4)_2\text{SO}_4)$ versus
530 ammonium bisulfate $(\text{NH}_4\text{HSO}_4)$ is relatively low and can occur within the 10 s time frame
531 (Robbins and Cadle, 1958; Daumer et al., 1992). A laboratory setting with ~5 ppbv NH_3 would

532 result in the filters needing to be exposed to laboratory air for at least 40 s to form ammonium
533 bisulfate (Fig. S8) versus the 3 to 10 s for conditions in the cabin of the DC-8 (Fig. 7), further
534 exemplifying the challenging conditions of the DC-8 cabin for filter sampling.

535 The prior analysis made the assumption that the PM maintained a spherical shape upon
536 impacting the Teflon filter. More viscous (i.e., solid) PM is more likely to maintain a spherical
537 shape on filters whereas less viscous (i.e., liquid) PM will spread and become more similar to
538 cylindrical shape (e.g., Slade et al., 2019). As more acidic aerosol is more likely to be liquid
539 (e.g., Murray and Bertram, 2008), an exploration of cylindrical shape was conducted. Depending
540 on the assumed height of the cylindrical shape, the timescale for a molecule of ammonia to
541 interact with a molecule of sulfuric acid decreases from ~5 s (for maximum ammonia and
542 aerosol volume) to ~4 s (assuming height of cylinder equals radius of sphere) to less than 1 s as
543 height decreases from 25 nm or less. The aerosol deforming and spreading upon impacting the
544 filters increases the particle surface area, and decreases the amount of time for cabin ammonium
545 to interact with the acidic PM. Thus, less viscous aerosol has more rapid uptake and interaction
546 with ammonia due to the higher surface area.

547 A potential limitation to the model is the accommodation coefficient of ammonia to
548 acidic PM, as there are conflicting reports on its value (Hanson and Kosciuch, 2004; Worsnop et
549 al., 2004). However, as shown in Worsnop et al. (2004), once the sulfuric acid weight percentage
550 is 50% or greater, the different studies converge to an accommodation coefficient of ~1. Various
551 studies indicate that the RH in the cabin of jet airplanes is low due to how air is brought into the
552 airplane, typically < 20% (Hunt and Space, 1994; Brundrett, 2001; National Research Council,
553 2002). Even though the ambient RH may be higher than the RH in the cabin of the DC-8, the

554 water equilibration is rapid (< 1 s) for the temperature of the cabin of the DC-8, even for very
555 viscous aerosol (Shiraiwa et al., 2011; Price et al., 2015; Ma et al., 2019), meaning the PM on the
556 filter would rapidly reach equilibrium with the cabin RH upon exposure. This would result in a \geq
557 60% sulfuric acid weight percentage (Wilson, 1921) for the typical RH ranges in the cabin of
558 typical airlines. However, various measurements in the DC-8 cabin indicate the RH is $\leq 40\%$
559 (Fig. S9), leading to sulfuric acid weight percentage of 50% or greater (Wilson, 1921).
560 Therefore, the accommodation coefficient of ~ 1 is well-constrained by the literature. Thus, the
561 handling of the filters between the sampling inlet to the polyethylene bag exposes the acidic PM
562 to enough gas-phase ammonia towards forming ammonium bisulfate or ammonium sulfate,
563 biasing high ammonium from the filters. This explains the differences seen in Fig. 1 – Fig. 4.

564 Another potential limitation is that the PM on the filters could form a layer, as multiple
565 particles pile up on top of each other, slowing the diffusion of ammonia to be taken up by acidic
566 PM. The filters have a one-sided surface area of $6.4 \times 10^{-3} \text{ m}^2$, while an individual particle at the
567 mode of the volume distribution (Fig. 7) has a projected surface area of $\sim 7.1 \times 10^{-14} \text{ m}^2$. Thus,
568 $\sim 9.0 \times 10^{10}$ particles would need to be collected to form a single layer of PM on the filter. The
569 number of molecules in a single particle of the mode size is $\sim 1.4 \times 10^8$ molecules (Eq. S2).
570 Therefore, $\sim 1.3 \times 10^{19}$ molecules need to be collected onto the filters in order to form a monolayer
571 of PM, which is equivalent to $\sim 2.2 \times 10^3 \text{ } \mu\text{g}$ total aerosol collected or $\sim 700 \text{ } \mu\text{g sm}^{-3}$ aerosol
572 concentration. As the mass concentration in ATom was typically $\sim 1 \text{ } \mu\text{g sm}^{-3}$ (Hodzic et al.,
573 2020), and total aerosol concentrations that high is rarely seen except for extreme events (such as
574 the thickest fresh wildfire plumes), it is very unlikely that more particle layering would delay the
575 diffusion of ammonia to acidic PM.

576 Various sensitivity analyses of the uptake of ammonia to sulfuric acid were conducted.
577 First, there is minimal impact of cabin temperature on the results. Though there was a 25 K range
578 in cabin temperature (Fig. S2), the impact on the molecular speed of ammonia in the model
579 (Eq. S1) leads to a $\pm 2\%$ change in molecular speed, resulting in small changes in the time.
580 Further, only large changes in the accommodation coefficient with temperature occurs for
581 sulfuric acid weight percentages $< 40\%$ (Swartz et al., 1999), which is smaller than the weight
582 percentage expected for the filters in the cabin of the DC-8. For the temperature range of the
583 cabin of the DC-8 (Fig. S2), the coefficient changes by less than 10%, which leads to a total
584 maximum change in Fig. 7 of $\pm 12\%$. The largest impact on the results in Fig. 7 is changing the
585 accommodation coefficient. Reducing the accommodation coefficient by a factor of 10, though
586 not representative of the DC-8 cabin conditions, would mean the acidic PM would need to be
587 exposed to ammonia for ≥ 1 minute (Fig. S10). It is expected that the lower accommodation
588 coefficient will occur for conditions with higher RH ($>80\%$), suggesting typical laboratory
589 conditions (along with the lower ammonia mixing ratios) or ambient conditions may experience
590 lower ammonia uptake to acidic PM. Finally, organic coatings may impact the accommodation
591 coefficient of ammonia to sulfuric acid; however, the amount of reduction on the accommodation
592 coefficient has varied among studies (e.g., Daumer et al., 1992; Liggio et al., 2011). Daumer et
593 al. (1992) showed no impact; whereas, Liggio et al. (2011) found a similar impact to reducing the
594 accommodation coefficient by a factor of 10 (Fig. S10). Thus, the results in Fig. 7 are in line
595 with Daumer et al. (1992) while the results in Fig. S10 are in line with Liggio et al. (2011).

596

597 **3.4 Impacts of Ammonia Uptake on Acidic Filters**

598 As discussed throughout this study, uptake of cabin ammonia during the handling of
599 acidic filters can lead to biases in ammonium mass concentrations. However, other potential
600 sources of biases include the material used for sampling and storing the filter (Hayes et al.,
601 1980), and the preparation of the filter in the field to be sampled by ion chromatography. As the
602 preparation of the filters occurs indoors, as well, the filters will be exposed to similar ammonia
603 mixing ratios to those shown in Fig. 6.

604 Further, filter collection of aerosols is a widely used technique outside of aircraft
605 campaigns, including for regulatory purposes and long-term monitoring at various locations
606 around the world. For many of these sites, ammonia denuders are used to minimize biases of
607 ammonium on filters (e.g., Baltensperger et al., 2003). Data from remote, high altitude locations
608 have indicated that the ammonium balance is less than one (Cozic et al., 2008; Sun et al., 2009;
609 Freney et al., 2016; Zhou et al., 2019), similar to the observations from the AMS shown in
610 Fig. 3. However, this is dependent on air mass origin and type (Cozic et al., 2008; Sun et al.,
611 2009; Fröhlich et al., 2015). Thus, sampling of remote aerosols with filters does provide
612 evidence of ammonium balances less than one due to a combination of procedures to minimize
613 interaction of gas-phase ammonia with the acidic filters and the lower human presence (and
614 potentially cooler temperatures at high, remote, mountaintop locations such as Jungfraujoch).

615 However, there are some long-term monitoring stations that do not use denuders or other
616 practices to minimize the interaction of ammonia with acidic aerosols. For example, the Clean
617 Air Status and Trends Network (CASTNET), which is located throughout the continental United
618 States, measures ammonium, sulfate, and nitrate (Solomon et al., 2014). The CASTNET system
619 uses an open-face system to collect aerosols on Teflon filters for approximately one week for

620 each filter (Lavery et al., 2009). In comparison, the Chemical Speciation Monitoring Network
621 (CSN), which also samples the continental United States and collects the aerosols on Nylon or
622 Teflon filters, a denuder is used to scrub gas-phase ammonia to minimize interaction of ammonia
623 with acidic aerosols on filters (Solomon et al., 2000, 2014). The comparison between these two
624 long-term monitoring sites show very different trends of ammonium balance versus total
625 inorganic mass concentration (Fig. S11). For CSN, the ammonium balance decreases with mass
626 concentration whereas CASTNET remains nearly constant. This is similar to the comparison
627 between SAGA and AMS in Fig. 4. This difference between the two sampling techniques may
628 be due to the lack of denuder in CASTNET to remove gas-phase ammonia. The use of the
629 denuders has led to CSN and other monitoring networks that use denuders to be more in-line
630 with in-situ observations (Kim et al., 2015; Weber et al., 2016). Further, as shown in Fig. S8,
631 exposure of an unprotected acidic filter for time greater than 1 day will lead to ammonia reacting
632 with the acid to form ammonium bisulfate or ammonium sulfate, even at low ammonia mixing
633 ratios. Other aspects that could impact this comparison, and are beyond the scope of this study
634 (but has been discussed in other studies (Hering and Cass, 1999; Schauer et al., 2003; Chow et
635 al., 2005, 2010; Dzepina et al., 2007; Watson et al., 2009; Nie et al., 2010; Liu et al., 2014, 2015;
636 Cheng and He, 2015; Heim et al., 2020)), include the loss of volatile ammonium from the
637 evaporation of ammonium nitrate or differences in the handling, shipping, and/or storage of the
638 filters or extracted samples. Thus, without denuders, or handling of filters with more than one
639 person present, will lead to similar differences between in-situ sampling versus filter collection
640 of inorganic aerosols observed during various aircraft campaigns.

641 Further, the uptake of ammonia onto acidic aerosols will impact comparisons with
642 chemical transport models (CTMs) and the understanding of various physical processes. For
643 example, various CTMs predict different results for the mass concentration of ammonium in the
644 upper troposphere (Wang et al., 2008a; Fisher et al., 2011; Ge et al., 2018), and selection of one
645 measurement versus the other will lead to different degrees of agreement. For example, for filters
646 that collect aerosols similar to those described here (no ammonia scrubber and/or exposed to
647 human emissions of ammonia), values of ammonium $< 0.2 \mu\text{g sm}^{-3}$ should be used with caution
648 or instead use *on-line* measurements of ammonium (specifically for SAGA measurements but a
649 similar analysis should be conducted for other filter-based measurements). This different
650 agreement impacts our understanding of important processes, such as the direct radiative impact
651 of inorganic aerosol (Wang et al., 2008b) or deposition of inorganic gases and aerosols (Nenes et
652 al., 2020a), as the gas-phase species have a faster deposition rate than the aerosol-phase. Finally,
653 the measurement biases can impact the suggested regulations to improve air quality (Nenes et al.,
654 2020b) and the calculated aerosol pH, as the pH is sensitive to the partitioning of ammonia
655 between the aerosol- and gas-phase (e.g., Hennigan et al., 2015).

656

657 **Conclusions**

658 Collection of aerosols onto filters to measure aerosol mass concentration and composition
659 is valuable for improving our understanding of the emissions and chemistry of inorganic aerosol,
660 and longstanding, multi-decadal filter-based records of atmospheric composition are invaluable
661 to analyze atmospheric change. However, as had been discussed in earlier studies, acidic aerosols
662 collected on filters are susceptible to uptake of gas-phase ammonia, which interacts with the

663 acidic aerosol to form an ammonium salt (e.g., ammonium bisulfate or ammonium sulfate). This
664 artifact in filter measurements can bias our understanding on the chemical composition of the
665 aerosol, which impacts numerous atmospheric processes.

666 We show that across six different aircraft campaigns, the aerosol collected on filters
667 showed a substantially higher ammonium mass concentration and ammonium balance compared
668 to AMS measurements. Further, another *on-line* measurement (PALMS) also shows lower
669 ammonium-to-sulfate ratios than for the filters. These differences are not due to differences in
670 the aerosol size ranges sampled by the PALMS and the filters. Instead, we show that the mixing
671 ratio of gas-phase ammonia in the cabin of the DC-8 is high enough (mean ~45 ppbv), and
672 similar to other indoor environments, to interact with acidic aerosol collected on filters in ≤ 10 s,
673 to form ammonium salts. These results are consistent with prior studies investigating this
674 interference. Thus, due to the interaction of ammonia in the cabin of research aircraft, we suggest
675 that a more realistic limit-of-detection of ammonium for the SAGA filters is 200 ng sm^{-3} , versus
676 the 10 ng sm^{-3} typically cited based on the ion chromatography measurement. Finally, even
677 though methods to reduce this bias have been implemented in several ground-based long-term
678 filter measurements of inorganic aerosols, there are still some networks that collect inorganic
679 aerosol without denuders to remove gas-phase ammonia, leading to similar discrepancies
680 between ground networks as observed between filters and AMS on the various aircraft
681 campaigns. Careful practice in both the aerosol collection and filtering handling is necessary to
682 better understand the emissions, chemistry, and chemical and physical properties of inorganic
683 aerosol.

684
685

686 Acknowledgements

687

688 This study was supported by NASA grants NNX15AH33A, NNX15AJ23G, 80NSSC18K0630,
689 and 80NSSC19K0124. We thank Glenn Diskin and the DACOM team for the use of the CO₂
690 measurements from FIREX-AQ, Armin Wisthaler for the use of the NH₃ measurements from
691 FIREX-AQ, Paul Wennberg for the use of HCN measurements from FIREX-AQ, Bruce
692 Anderson, Luke Ziemba, and the LARGE team for the use of the LAS volume distribution from
693 SEAC⁴RS, Karl Froyd, Gregory Schill, and Daniel Murphy for the use of the PALMS
694 observations from ATom-1 and -2, and Charles Brock, Agnieszka Kupc, and Christina
695 Williamson for the volume distribution measurements during ATom-1 and -2. Also, we thank J.
696 Andrew Neuman for the use of the Picarro G2103 during FIREX-AQ. We thank the crew of the
697 DC-8 and C-130 aircraft for extensive support in the field deployments. We specifically thank
698 Adam Webster and the crew of the NASA DC-8 in their assistance and persistence in allowing us
699 to install the Picarro G2103 during FIREX-AQ in order to measure ammonia in the cabin.

700

701 Data Availability

702

703 ARCTAS-A and -B measurements are available at
704 <http://doi.org/10.5067/SUBORBITAL/ARCTAS2008/DATA001>, last access 27 April 2020.
705 SEAC⁴RS measurements are available at
706 <http://doi.org/10.5067/Aircraft/SEAC4RS/Aerosol-TraceGas-Cloud>, last access 27 April 2020.
707 WINTER measurements are available at https://data.eol.ucar.edu/master_lists/generated/winter/,
708 last access 27 April 2020. ATom-1 and -2 measurements are available at
709 <https://doi.org/10.3334/ORNLDAAAC/1581>, last access 27 April 2020. Ammonia and carbon
710 dioxide measurements from the cabin of the DC-8 are available as an attachment . CSN and
711 CASTNET measurements are available at
712 <http://views.cira.colostate.edu/fed/QueryWizard/Default.aspx>, last access 27 April 2020. Figures
713 are available at http://cires1.colorado.edu/jimenez/group_pubs.html.

714

715 Competing Interests

716 The authors declare no competing interests.

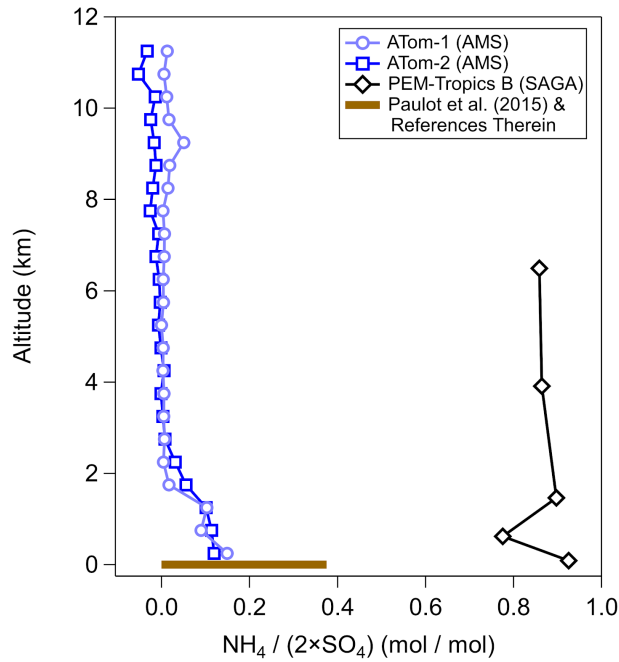
717

718 Author Contribution

719 B.A.N., P.C.-J., D.A.D., and J.L.J. designed the experiment and wrote the paper. B.A.N., P.C.-J.,
720 D.A.D., H.G., A.V.H., D.P., J.C.S., M.K.S., M.J.C., J.E.D., W.H., and B.B.P. collected and
721 analyzed the data. D.S.J. and A.H. ran GEOS-Chem and provided the output. All authors
722 reviewed the paper.

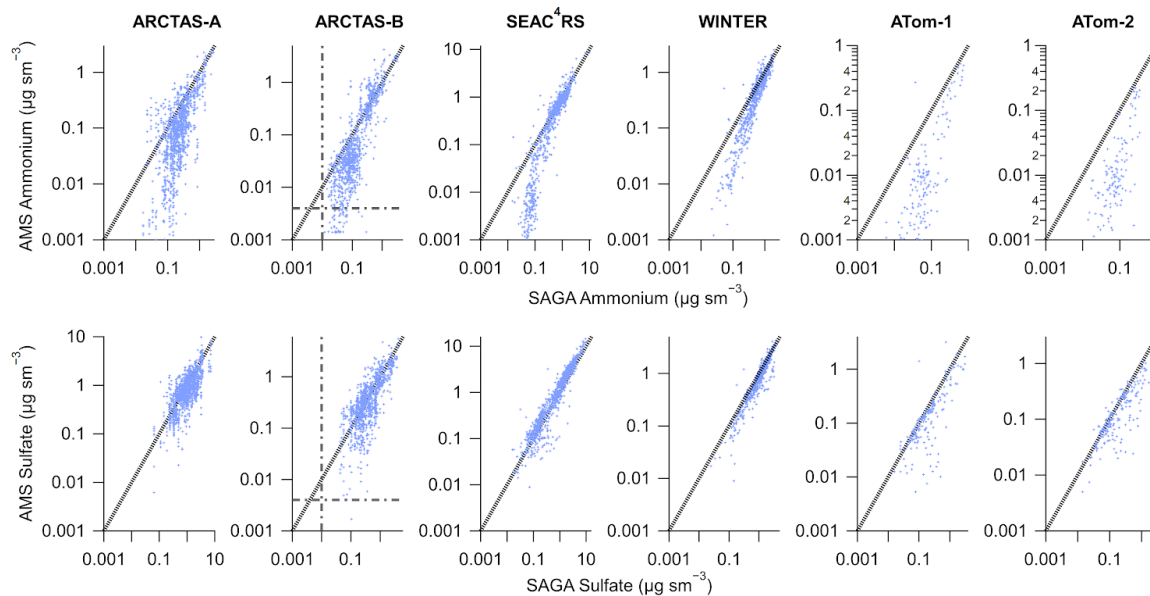
723 **Figures**

724



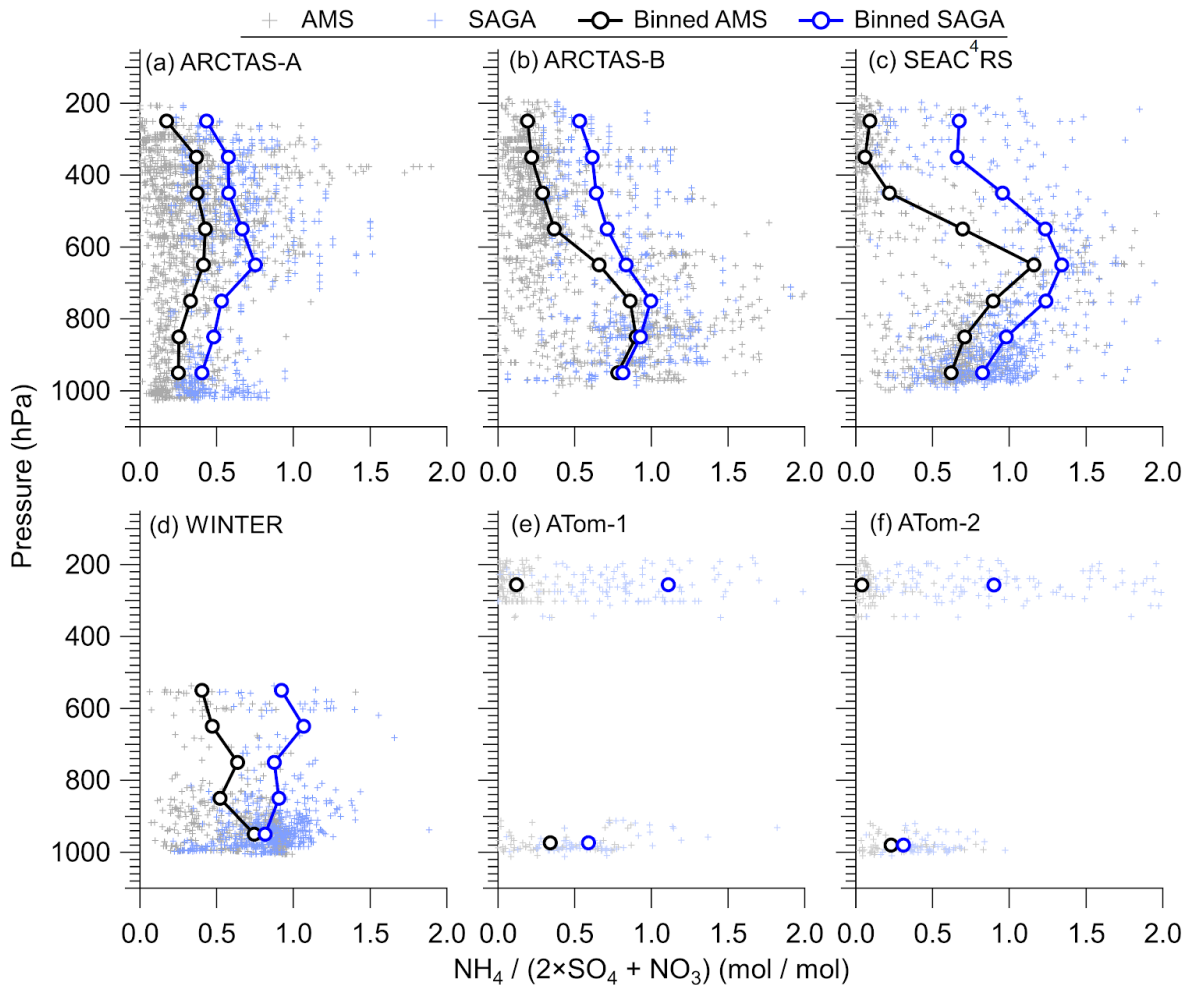
725 Figure 1. Vertical profile of sulfate-only ion molar balance ($moles(NH_4)/moles(SO_4)$) measured
 726 during PEM-Tropics by collecting the aerosol on filters and analyzing it off-line with ion
 727 chromatography (Dibb et al., 2002) and during ATom-1 and -2 by AMS (Hodzic et al., 2020).
 728 The ammonium balance profile is for observations collected during ATom-1 and -2 between
 729 $-20^\circ S$ and $20^\circ N$ in the Pacific basin, so that the observations were in a similar location as the
 730 PEM-Tropics samples. Also shown is the ammonium balance from observations summarized in
 731 Paulot et al. (2015), and reference therein, for the area around the same location as
 732 PEM-Tropics.

733



734

735 Figure 2. Scatter plot of AMS (y-axis) versus SAGA filter (x-axis) ammonium (top) and sulfate
 736 (bottom) mass concentration from 6 different aircraft campaigns. AMS data have been averaged
 737 over the SAGA filter collection times. Black line is the one-to-one line and the grey dash-dot
 738 lines are the estimated detection limits for AMS (DeCarlo et al., 2006; Guo et al., 2020) at the
 739 SAGA filter collection interval (~5 minutes) and the estimated detection limits for SAGA (Dibb et
 740 al., 1999). Data has been averaged to the sampling time of SAGA and has not been filtered for
 741 supermicron particles. For ATom-1 and -2, data during ascent and descent has been removed
 742 (only level sampling at low altitude and high altitude).

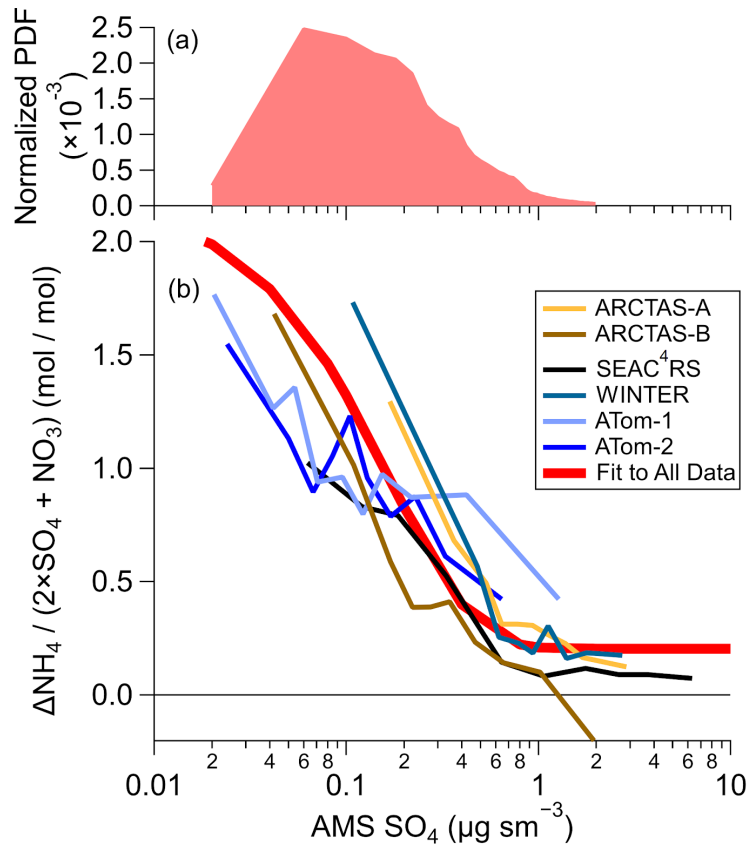


743

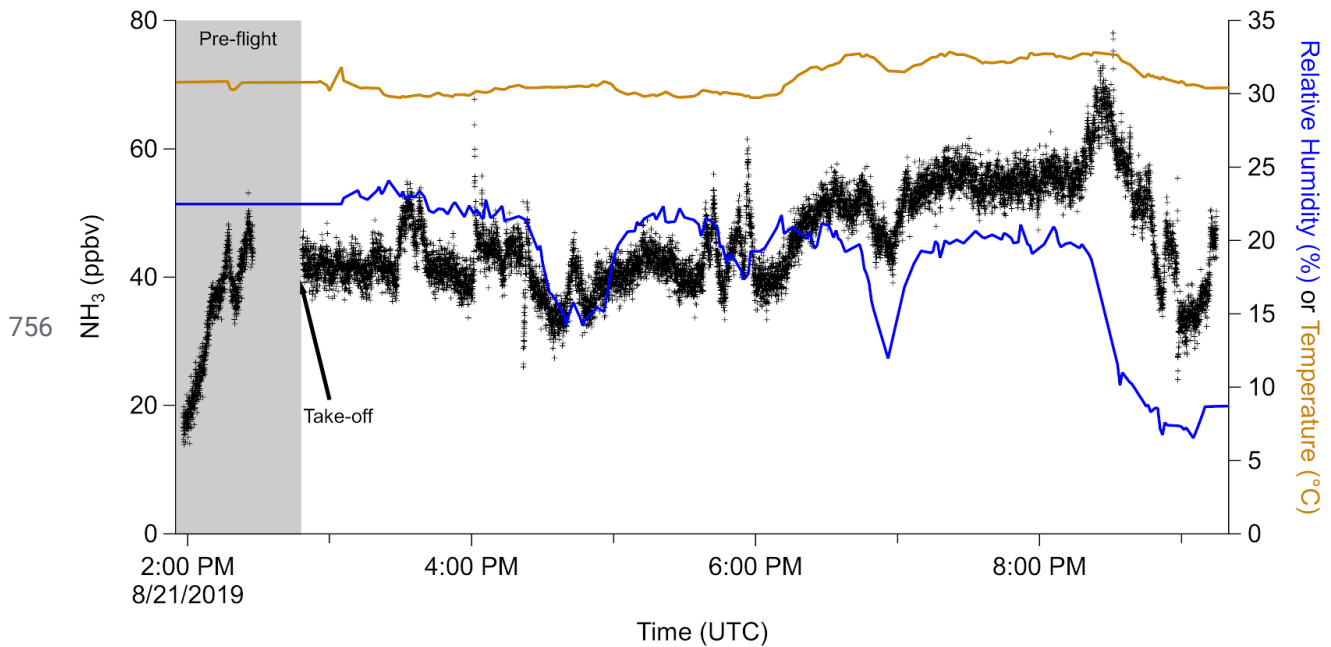
744 Figure 3. Vertical profiles of ammonium balance $((NH_4/18)/(2 \times SO_4/96 + NO_3/62))$ for (a)
 745 ARCTAS-A, (b) ARCTAS-B, (c) SEAC⁴RS, (d) WINTER, (e) ATom-1, and (f) ATom-2, for AMS
 746 and SAGA. The binned data is the mean for each 100 hPa pressure level. The data has been
 747 averaged to the sampling time of SAGA filters.

748

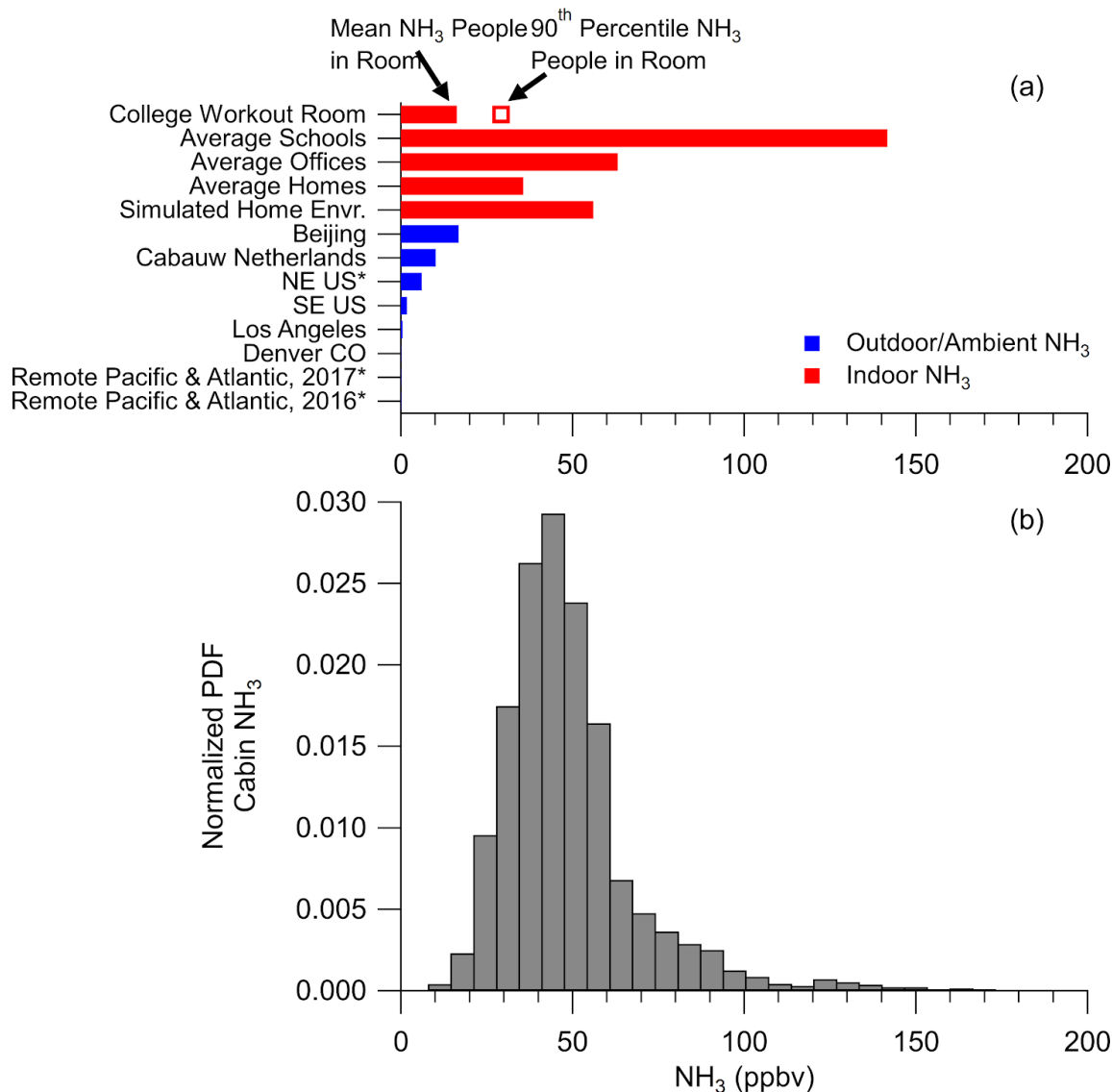
749



750 Figure 4. (a) Predicted normalized probability distribution function (PDF) for tropospheric
 751 (pressure > 250 hPa) sulfate from GEOS-Chem for one model year (see SI). (b) Difference
 752 between SAGA and AMS ammonium, in mol sm^{-3} , divided by AMS sulfate and nitrate, in mol
 753 sm^{-3} , versus AMS sulfate ($\mu\text{g sm}^{-3}$), for the six different airborne campaigns. The values shown
 754 are binned deciles for the five different airborne campaigns. The fit shown in (b) is for all data
 755 from all campaigns.

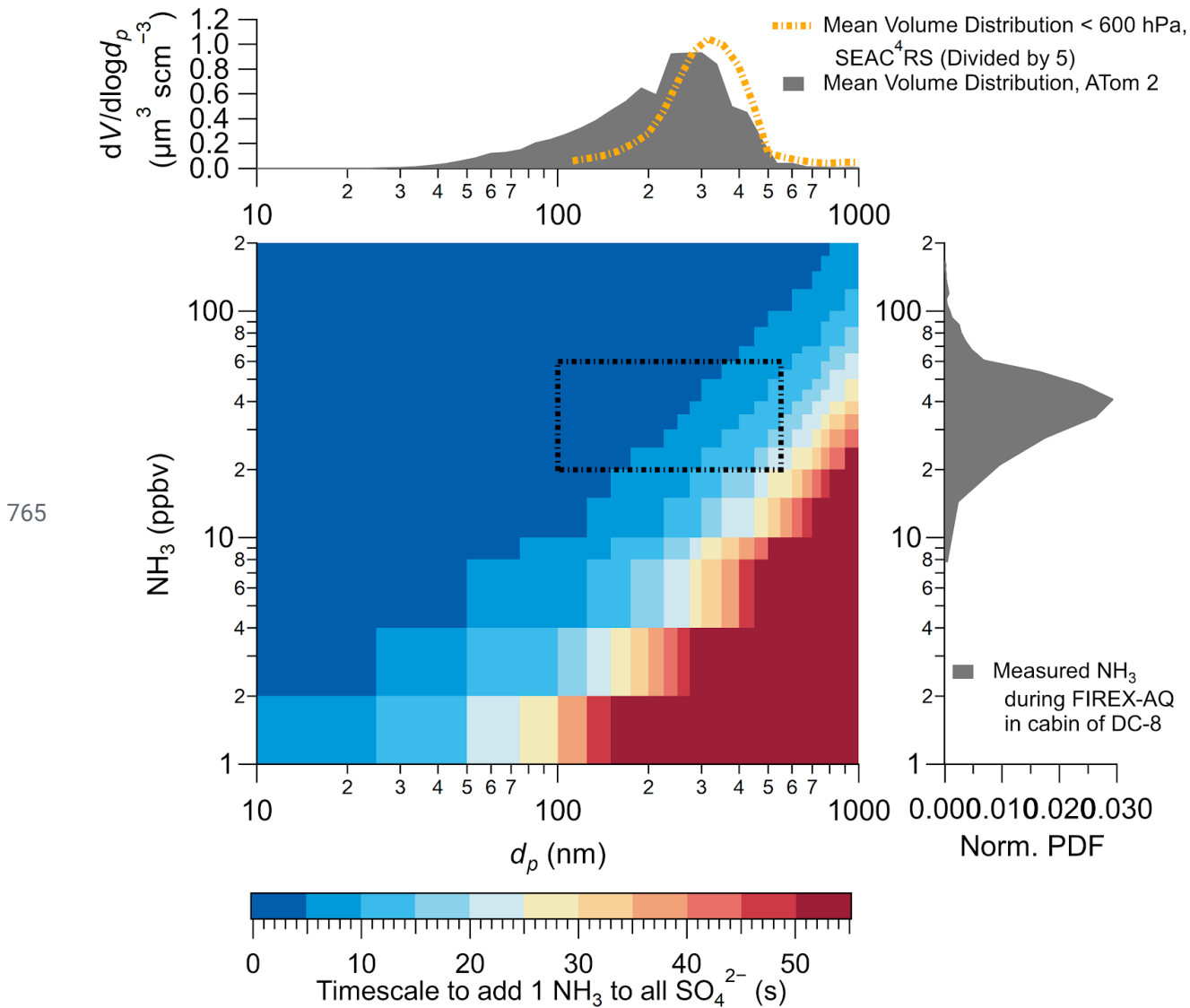


757 Figure 5. Time series of ammonia (left) and relative humidity and temperature (right) measured
 758 inside the cabin of the NASA DC-8 during a flight during the FIREX-AQ campaign. Time spent
 759 prior to take-off is marked with a grey background.



760

761 Figure 6. (a) Ammonia (NH_3) (ppbv) reported for studies. See Table S1 for references. Asterisk
 762 after study name indicates NH_3 predicted by thermodynamic model instead of being measured.
 763 (b) Normalized probability distribution function (PDF) for NH_3 , measured in the cabin of the
 764 NASA DC-8 during FIREX-AQ.



771 References

- 772 Abbatt, J. P. D., Benz, S., Cziczo, D. J., Kanji, Z., Lohmann, U. and Möhler, O.: Solid
773 ammonium sulfate aerosols as ice nuclei: a pathway for cirrus cloud formation, *Science*,
774 313(5794), 1770–1773, 2006.
- 775 Aknan, A.: NASA Airborne Science Data for Atmospheric Composition, TABMEP2
776 POLARCAT Preliminary Assessment Reports [online] Available from:
777 <http://www-air.larc.nasa.gov/> (Accessed 3 June 2020), 2015.
- 778 Ampollini, L., Katz, E. F., Bourne, S., Tian, Y., Novoselac, A., Goldstein, A. H., Lucic, G.,
779 Waring, M. S. and DeCarlo, P. F.: Observations and Contributions of Real-Time Indoor
780 Ammonia Concentrations during HOMEChem, *Environ. Sci. Technol.*, 53(15), 8591–8598,
781 2019.
- 782 Bahreini, R., Dunlea, E. J., Matthew, B. M., Simons, C., Docherty, K. S., DeCarlo, P. F., Jimenez,
783 J. L., Brock, C. A. and Middlebrook, A. M.: Design and Operation of a Pressure-Controlled Inlet
784 for Airborne Sampling with an Aerodynamic Aerosol Lens, *Aerosol Sci. Technol.*, 42(6),
785 465–471, 2008.
- 786 Bahreini, R., Ervens, B., Middlebrook, A. M., Warneke, C., De Gouw, J. A., DeCarlo, P. F.,
787 Jimenez, J. L., Brock, C. A., Neuman, J. A., Ryerson, T. B., Stark, H., Atlas, E., Brioude, J.,
788 Fried, A., Holloway, J. S., Peischl, J., Richter, D., Walega, J., Weibring, P., Wollny, A. G. and
789 Fehsenfeld, F. C.: Organic aerosol formation in urban and industrial plumes near Houston and
790 Dallas, Texas, *J. Geophys. Res. D: Atmos.*, 114(16), 1–17, 2009.
- 791 Baltensperger, U., Barrie, L., Frohlich, C., Gras, J., Jäger, H., Jennings, S. G., Li, S.-M., Ogren,
792 J., Widensohler, A., Wehrli, C. and Wilson, J.: WMO/GAW Aerosol Measurement Procedures
793 Guidelines and Recommendations, WMO GAW. [online] Available from:
794 https://library.wmo.int/doc_num.php?explnum_id=9244, 2003.
- 795 von Bobruzki, K., Braban, C. F., Famulari, D., Jones, S. K., Blackall, T., Smith, T. E. L., Blom,
796 M., Coe, H., Gallagher, M., Ghalaieny, M., McGillen, M. R., Percival, C. J., Whitehead, J. D.,
797 Ellis, R., Murphy, J., Mohacsi, A., Pogany, A., Junninen, H., Rantanen, S., Sutton, M. A. and
798 Nemitz, E.: Field inter-comparison of eleven atmospheric ammonia measurement techniques,
799 *Atmos. Meas. Tech.*, 3(1), 91–112, 2010.
- 800 Brock, C. A., Williamson, C., Kupc, A., Froyd, K. D., Erdesz, F., Wagner, N., Richardson, M.,
801 Schwarz, J. P., Gao, R.-S., Katich, J. M., Campuzano-Jost, P., Nault, B. A., Schroder, J. C.,
802 Jimenez, J. L., Weinzierl, B., Dollner, M., Bui, T. and Murphy, D. M.: Aerosol size distributions
803 during the Atmospheric Tomography Mission (ATom): methods, uncertainties, and data products,
804 *Atmos. Meas. Tech.*, 12(6), 3081–3099, 2019.
- 805 Brundrett, G.: Comfort and health in commercial aircraft: a literature review, *J. R. Soc. Promot.*
806 *Health*, 121(1), 29–37, 2001.
- 807 Canagaratna, M. R., Jayne, J. T., Jimenez, J. L., Allan, J. D., Alfarra, M. R., Zhang, Q., Onasch,

808 T. B., Drewnick, F., Coe, H., Middlebrook, A., Delia, A., Williams, L. R., Trimborn, A. M.,
809 Northway, M. J., DeCarlo, P. F., Kolb, C. E., Davidovits, P. and Worsnop, D. R.: Chemical and
810 microphysical characterization of ambient aerosols with the aerodyne aerosol mass spectrometer,
811 *Mass Spectrom. Rev.*, 26(2), 185–222, 2007.

812 Cheng, Y. and He, K.-B.: Measurement of carbonaceous aerosol with different sampling
813 configurations and frequencies, *Atmos. Meas. Tech.*, 8(7), 2639–2648, 2015.

814 Chow, J. C., Watson, J. G., Lowenthal, D. H. and Magliano, K. L.: Loss of PM_{2.5} Nitrate from
815 Filter Samples in Central California, *J. Air Waste Manage. Assoc.*, 55(8), 1158–1168, 2005.

816 Chow, J. C., Watson, J. G., Chen, L.-W. A., Rice, J. and Frank, N. H.: Quantification of PM_{2.5}
817 organic carbon sampling artifacts in US networks, *Atmos. Chem. Phys.*, 10(12), 5223–5239,
818 2010.

819 Clark, K. W., Anderson, K. R., Linn, W. S. and Gong, H., Jr: Influence of breathing-zone
820 ammonia on human exposures to acid aerosol pollution, *J. Air Waste Manag. Assoc.*, 45(11),
821 923–925, 1995.

822 Cohen, A. J., Brauer, M., Burnett, R., Anderson, H. R., Frostad, J., Estep, K., Balakrishnan, K.,
823 Brunekreef, B., Dandona, L., Dandona, R., Feigin, V., Freedman, G., Hubbell, B., Jobling, A.,
824 Kan, H., Knibbs, L., Liu, Y., Martin, R., Morawska, L., Pope, C. A., Shin, H., Straif, K.,
825 Shaddick, G., Thomas, M., van Dingenen, R., van Donkelaar, A., Vos, T., Murray, C. J. L. and
826 Forouzanfar, M. H.: Estimates and 25-year trends of the global burden of disease attributable to
827 ambient air pollution: an analysis of data from the Global Burden of Diseases Study 2015,
828 *Lancet*, 389(10082), 1907–1918, 2017.

829 Colberg, C. A., Luo, B. P., Wernli, H., Koop, T. and Peter, T.: A novel model to predict the
830 physical state of atmospheric H₂SO₄/NH₃/H₂O aerosol particles, *Atmos. Chem. Phys.*, 3(4),
831 909–924, 2003.

832 Coury, C. and Dillner, A. M.: ATR-FTIR characterization of organic functional groups and
833 inorganic ions in ambient aerosols at a rural site, *Atmos. Environ.*, 43(4), 940–948, 2009.

834 Cozic, J., Verheggen, B., Weingartner, E., Crosier, J., Bower, K. N., Flynn, M., Coe, H.,
835 Henning, S., Steinbacher, M., Henne, S., Collaud Coen, M., Petzold, A. and Baltensperger, U.:
836 Chemical composition of free tropospheric aerosol for PM₁ and coarse mode at the high alpine
837 site Jungfraujoch, *Atmos. Chem. Phys.*, 8(2), 407–423, 2008.

838 Cubison, M. J., Ortega, A. M., Hayes, P. L., Farmer, D. K., Day, D. A., Lechner, M. J., Brune, W.
839 H., Apel, E., Diskin, G. S., Fisher, J. A., Fuelberg, H. E., Hecobian, A., Knapp, D. J., Mikoviny,
840 T., Riemer, D., Sachse, G. W., Sessions, W., Weber, R. J., Weinheimer, A. J., Wisthaler, A. and
841 Jimenez, J. L.: Effects of aging on organic aerosol from open biomass burning smoke in aircraft
842 and laboratory studies, *Atmos. Chem. Phys.*, 11(23), 12049–12064, 2011.

843 Daumer, B., Niessner, R. and Klockow, D.: Laboratory studies of the influence of thin organic
844 films on the neutralization reaction of H₂SO₄ aerosol with ammonia, *J. Aerosol Sci.*, 23(4),

845 315–325, 1992.

846 DeCarlo, P. F., Kimmel, J. R., Trimborn, A., Northway, M. J., Jayne, J. T., Aiken, A. C., Gonin,
847 M., Fuhrer, K., Horvath, T., Docherty, K. S., Worsnop, D. R. and Jimenez, J. L.:
848 Field-deployable, high-resolution, time-of-flight aerosol mass spectrometer, *Anal. Chem.*,
849 78(24), 8281–8289, 2006.

850 DeCarlo, P. F., Dunlea, E. J., Kimmel, J. R., Aiken, A. C., Sueper, D., Crounse, J., Wennberg, P.
851 O., Emmons, L., Shinozuka, Y., Clarke, A., Zhou, J., Tomlinson, J., Collins, D. R., Knapp, D.,
852 Weinheimer, A. J., Montzka, D. D., Campos, T. and Jimenez, J. L.: Fast airborne aerosol size and
853 chemistry measurements above Mexico City and Central Mexico during the MILAGRO
854 campaign, *Atmos. Chem. Phys.*, 8(14), 4027–4048, 2008.

855 Dentener, F. J. and Crutzen, P. J.: A three-dimensional model of the global ammonia cycle, *J.*
856 *Atmos. Chem.*, 19(4), 331–369, 1994.

857 Dibb, J. E., Talbot, R. W., Scheuer, E. M., Blake, D. R., Blake, N. J., Gregory, G. L., Sachse, G.
858 W. and Thornton, D. C.: Aerosol chemical composition and distribution during the Pacific
859 Exploratory Mission (PEM) Tropics, *J. Geophys. Res.*, 104(D5), 5785–5800, 1999.

860 Dibb, J. E., Talbot, R. W. and Scheuer, E. M.: Composition and distribution of aerosols over the
861 North Atlantic during the Subsonic Assessment Ozone and Nitrogen Oxide Experiment
862 (SONEX), *J. Geophys. Res. D: Atmos.*, 105(D3), 3709–3717, 2000.

863 Dibb, J. E., Talbot, R. W., Seid, G., Jordan, C., Scheuer, E., Atlas, E., Blake, N. J. and Blake, D.
864 R.: Airborne sampling of aerosol particles: Comparison between surface sampling at Christmas
865 Island and P-3 sampling during PEM-Tropics B, *J. Geophys. Res.*, 108(D2), 11335, 2002.

866 Dibb, J. E., Talbot, R. W., Scheuer, E. M., Seid, G., Avery, M. A. and Singh, H. B.: Aerosol
867 chemical composition in Asian continental outflow during the TRACE-P campaign: Comparison
868 with PEM-West B, *J. Geophys. Res.: Atmos.*, 108(D21), 8815, 2003.

869 Dzepina, K., Arey, J., Marr, L. C., Worsnop, D. R., Salcedo, D., Zhang, Q., Onasch, T. B.,
870 Molina, L. T., Molina, M. J. and Jimenez, J. L.: Detection of particle-phase polycyclic aromatic
871 hydrocarbons in Mexico City using an aerosol mass spectrometer, *Int. J. Mass Spectrom.*, 263(2),
872 152–170, 2007.

873 Faloon, I.: Sulfur processing in the marine atmospheric boundary layer: A review and critical
874 assessment of modeling uncertainties, *Atmos. Environ.*, 43(18), 2841–2854, 2009.

875 Filges, A., Gerbig, C., Rella, C. W., Hoffnagle, J., Smit, H., Krämer, M., Spelten, N., Rolf, C.,
876 Bozóki, Z., Buchholz, B. and Ebert, V.: Evaluation of the IAGOS-Core GHG package H₂O
877 measurements during the DENCHAR airborne inter-comparison campaign in 2011, *Atmos.*
878 *Meas. Tech.*, 11(9), 5279–5297, 2018.

879 Finewax, Z., Pagonis, D., Claflin, M. S., Handschy, A. V., Brown, W. L., Ba, J. O. N., Lerner, B.
880 M., Jimenez, J. L., Ziemann, P. J. and de Gouw, J. A.: Quantification and source characterization

of volatile organic compounds from exercising and application of chlorine-based cleaning products in a university athletic center, *Indoor Air*, Submitted, 2020.

Fisher, J. A., Jacob, D. J., Wang, Q., Bahreini, R., Carouge, C. C., Cubison, M. J., Dibb, J. E., Diehl, T., Jimenez, J. L., Leibensperger, E. M., Lu, Z., Meinders, M. B. J., Pye, H. O. T., Quinn, P. K., Sharma, S., Streets, D. G., van Donkelaar, A. and Yantosca, R. M.: Sources, distribution, and acidity of sulfate–ammonium aerosol in the Arctic in winter–spring, *Atmos. Environ.*, 45(39), 7301–7318, 2011.

Freney, E., Sellegri Karine, S. K., Eija, A., Clemence, R., Aurelien, C., Jean-Luc, B., Aurelie, C., Hervo Maxime, H. M., Nadege, M., Laeticia, B. and David, P.: Experimental Evidence of the Feeding of the Free Troposphere with Aerosol Particles from the Mixing Layer, *Aerosol Air Qual. Res.*, 16(3), 702–716, 2016.

Fröhlich, R., Cubison, M. J., Slowik, J. G., Bukowiecki, N., Canonaco, F., Croteau, P. L., Gysel, M., Henne, S., Herrmann, E., Jayne, J. T., Steinbacher, M., Worsnop, D. R., Baltensperger, U. and Prévôt, A. S. H.: Fourteen months of on-line measurements of the non-refractory submicron aerosol at the Jungfraujoch (3580 m a.s.l.) – chemical composition, origins and organic aerosol sources, *Atmos. Chem. Phys.*, 15(19), 11373–11398, 2015.

Froyd, K. D., Murphy, D. M., Sanford, T. J., Thomson, D. S., Wilson, J. C., Pfister, L. and Lait, L.: Aerosol composition of the tropical upper troposphere, *Atmos. Chem. Phys.*, 9(13), 4363–4385, 2009.

Froyd, K. D., Murphy, D. M., Brock, C. A., Campuzano-Jost, P., Dibb, J. E., Jimenez, J.-L., Kupc, A., Middlebrook, A. M., Schill, G. P., Thornhill, K. L., Williamson, C. J., Wilson, J. C. and Ziemba, L. D.: A new method to quantify mineral dust and other aerosol species from aircraft platforms using single-particle mass spectrometry, *Atmos. Meas. Tech.*, 12(11), 6209–6239, 2019.

Fuchs, N. A. and Sutugin, A. G.: High-Dispersed Aerosols, in *Topics in Current Aerosol Research*, edited by G. M. Hidy and J. R. Brock, Pergamon., 1971.

Ge, C., Zhu, C., Francisco, J. S., Zeng, X. C. and Wang, J.: A molecular perspective for global modeling of upper atmospheric NH₃ from freezing clouds, *Proc. Natl. Acad. Sci. U. S. A.*, 115(24), 6147–6152, 2018.

Guo, H., Xu, L., Bougiatioti, A., Cerully, K. M., Capps, S. L., Hite, J. R., Carlton, A. G., Lee, S.-H., Bergin, M. H., Ng, N. L., Nenes, A. and Weber, R. J.: Fine-particle water and pH in the southeastern United States, *Atmos. Chem. Phys.*, 15(9), 5211–5228, 2015.

Guo, H., Sullivan, A. P., Campuzano-Jost, P., Schroder, J. C., Lopez-Hilfiker, F. D., Dibb, J. E., Jimenez, J. L., Thornton, J. A., Brown, S. S., Nenes, A. and Weber, R. J.: Fine particle pH and the partitioning of nitric acid during winter in the northeastern United States, *J. Geophys. Res. D: Atmos.*, 121(17), 10,355–10,376, 2016.

Guo, H., Nenes, A. and Weber, R. J.: The underappreciated role of nonvolatile cations in aerosol

ammonium-sulfate molar ratios, *Atmos. Chem. Phys.*, 18(23), 17307–17323, 2018.

Guo, H., Campuzano-Jost, P., Nault, B. A., Day, D. A., Schroder, J. C., Dibb, J. E., Dollner, M., Weinzierl, B. and Jimenez, J. L.: The Importance of Size Ranges in Intercomparison of Aerosol Volume Concentration Measurements: A Case Study for Aerosol Mass Spectrometer in the ATom Mission, *Atmos. Meas. Tech. Discuss.*, In Review, doi:10.5194/amt-2020-224, 2020.

Hanson, D. and Kosciuch, E.: The NH₃ Mass Accommodation Coefficient for Uptake onto Sulfuric Acid Solutions, *J. Phys. Chem. A*, 107(13), 2199–2208, 2003.

Hanson, D. R. and Kosciuch, E.: Reply to “Comment on ‘The NH₃ Mass Accommodation Coefficient for Uptake onto Sulfuric Acid Solutions,’” *J. Phys. Chem. A*, 108(40), 8549–8551, 2004.

Hayes, D., Snetsinger, K., Ferry, G., Oberbeck, V. and Farlow, N.: Reactivity of stratospheric aerosols to small amounts of ammonia in the laboratory environment, *Geophys. Res. Lett.*, 7(11), 974–976, 1980.

Heald, C. L. and Kroll, J. H.: The fuel of atmospheric chemistry: Toward a complete description of reactive organic carbon, *Sci Adv*, 6(6), eaay8967, 2020.

Heald, C. L., Collett, J. L., Jr., Lee, T., Benedict, K. B., Schwandner, F. M., Li, Y., Clarisse, L., Hurtmans, D. R., Van Damme, M., Clerbaux, C., Coheur, P.-F., Philip, S., Martin, R. V. and Pye, H. O. T.: Atmospheric ammonia and particulate inorganic nitrogen over the United States, *Atmos. Chem. Phys.*, 12(21), 10295–10312, 2012.

Heim, E. W., Dibb, J., Scheuer, E., Jost, P. C., Nault, B. A., Jimenez, J. L., Peterson, D., Knote, C., Fenn, M., Hair, J., Beyersdorf, A. J., Corr, C. and Anderson, B. E.: Asian dust observed during KORUS-AQ facilitates the uptake and incorporation of soluble pollutants during transport to South Korea, *Atmos. Environ.*, 224, 117305, 2020.

Hennigan, C. J., Sullivan, A. P., Fountoukis, C. I., Nenes, A., Hecobian, A., Vargas, O., Peltier, R. E., Hanks, A. T. C., Huey, L. G., Lefer, B. L., Russell, A. G. and Weber, R. J.: On the volatility and production mechanisms of newly formed nitrate and water soluble organic aerosol in Mexico City, *Atmos. Chem. Phys.*, 8(14), 3761–3768, 2008.

Hennigan, C. J., Izumi, J., Sullivan, A. P., Weber, R. J. and Nenes, A.: A critical evaluation of proxy methods used to estimate the acidity of atmospheric particles, *Atmos. Chem. Phys.*, 15(5), 2775–2790, 2015.

Henze, D. K., Seinfeld, J. H. and Shindell, D. T.: Inverse modeling and mapping US air quality influences of inorganic PM_{2.5} precursor emissions using the adjoint of GEOS-Chem, *Atmos. Chem. Phys.*, 9(16), 5877–5903, 2009.

Hering, S. and Cass, G.: The Magnitude of Bias in the Measurement of PM₂₅ Arising from Volatilization of Particulate Nitrate from Teflon Filters, *J. Air Waste Manag. Assoc.*, 49(6),

725–733, 1999.

Hocking, M. B.: Indoor air quality: recommendations relevant to aircraft passenger cabins, *Am. Ind. Hyg. Assoc. J.*, 59(7), 446–454, 1998.

Hodzic, A. and Duvel, J. P.: Impact of Biomass Burning Aerosols on the Diurnal Cycle of Convective Clouds and Precipitation Over a Tropical Island: Fire aerosols effect on deep convection, *J. Geophys. Res. D: Atmos.*, 123(2), 1017–1036, 2018.

Hodzic, A., Campuzano-Jost, P., Bian, H., Chin, M., Colarco, P. R., Day, D. A., Froyd, K. D., Heinold, B., Jo, D. S., Katich, J. M., Kodros, J. K., Nault, B. A., Pierce, J. R., Ray, E., Schacht, J., Schill, G. P., Schroder, J. C., Schwarz, J. P., Sueper, D. T., Tegen, I., Tilmes, S., Tsigaridis, K., Yu, P. and Jimenez, J. L.: Characterization of Organic Aerosol across the Global Remote Troposphere: A comparison of ATom measurements and global chemistry models, *Atmos. Chem. Phys.*, 20(8), 4607–4635, 2020.

Hunt, E. W. and Space, D. R.: The Airplane Cabin Environment: Issues Pertaining to Flight Attendant, in *Comfort*,” International in-flight Service Management Organization Conference. [online] Available from: <http://citeseerx.ist.psu.edu/viewdoc/similar?doi=10.1.1.304.7321&type=cc> (Accessed 25 March 2020), 1994.

Huntzicker, J. J., Cary, R. A. and Ling, C.-S.: Neutralization of sulfuric acid aerosol by ammonia, *Environ. Sci. Technol.*, 14(7), 819–824, 1980.

Hu, W., Hu, M., Hu, W., Jimenez, J. L., Yuan, B., Chen, W., Wang, M., Wu, Y., Chen, C., Wang, Z., Peng, J., Zeng, L. and Shao, M.: Chemical composition, sources, and aging process of submicron aerosols in Beijing: Contrast between summer and winter, *J. Geophys. Res. D: Atmos.*, 121(4), 1955–1977, 2016.

Hu, W., Campuzano-Jost, P., Day, D. A., Croteau, P., Canagaratna, M. R., Jayne, J. T., Worsnop, D. R. and Jimenez, J. L.: Evaluation of the new capture vaporizer for aerosol mass spectrometers (AMS) through field studies of inorganic species, *Aerosol Sci. Technol.*, 51(6), 735–754, 2017a.

Hu, W., Campuzano-Jost, P., Day, D. A., Croteau, P., Canagaratna, M. R., Jayne, J. T., Worsnop, D. R. and Jimenez, J. L.: Evaluation of the new capture vapourizer for aerosol mass spectrometers (AMS) through laboratory studies of inorganic species, *Atmospheric Measurement Techniques*, 10(6), 2897–2921, 2017b.

Hu, W., Campuzano-Jost, P., Day, D. A., Nault, B. A., Park, T., Lee, T., Pajunoja, A., Virtanen, A., Croteau, P., Canagaratna, M. R., Jayne, J. T., Worsnop, D. R. and Jimenez, J. L.: Ambient Quantification and Size Distributions for Organic Aerosol in Aerosol Mass Spectrometers with the New Capture Vaporizer, *ACS Earth Space Chem.*, doi:10.1021/acsearthspacechem.9b00310, 2020.

Jacob, D. J., Crawford, J. H., Maring, H., Clarke, A. D., Dibb, J. E., Emmons, L. K., Ferrare, R. A., Hostetler, C. A., Russell, P. B., Singh, H. B., Thompson, A. M., Shaw, G. E., McCauley, E.,

Pederson, J. R. and Fisher, J. A.: The Arctic Research of the Composition of the Troposphere from Aircraft and Satellites (ARCTAS) mission: design, execution, and first results, *Atmos. Chem. Phys.*, 10(11), 5191–5212, 2010.

Jimenez, J. L., Canagaratna, M. R., Donahue, N. M., Prevot, A. S. H., Zhang, Q., Kroll, J. H., DeCarlo, P. F., Allan, J. D., Coe, H., Ng, N. L., Aiken, A. C., Docherty, K. S., Ulbrich, I. M., Grieshop, A. P., Robinson, A. L., Duplissy, J., Smith, J. D., Wilson, K. R., Lanz, V. A., Hueglin, C., Sun, Y. L., Tian, J., Laaksonen, A., Raatikainen, T., Rautiainen, J., Vaattovaara, P., Ehn, M., Kulmala, M., Tomlinson, J. M., Collins, D. R., Cubison, M. J., Dunlea, E. J., Huffman, J. A., Onasch, T. B., Alfarra, M. R., Williams, P. I., Bower, K., Kondo, Y., Schneider, J., Drewnick, F., Borrmann, S., Weimer, S., Demerjian, K., Salcedo, D., Cottrell, L., Griffin, R., Takami, A., Miyoshi, T., Hatakeyama, S., Shimono, A., Sun, J. Y., Zhang, Y. M., Dzepina, K., Kimmel, J. R., Sueper, D., Jayne, J. T., Herndon, S. C., Trimborn, A. M., Williams, L. R., Wood, E. C., Middlebrook, A. M., Kolb, C. E., Baltensperger, U. and Worsnop, D. R.: Evolution of organic aerosols in the atmosphere, *Science*, 326(5959), 1525–1529, 2009.

Kamp, J. N., Chowdhury, A., Adamsen, A. P. S. and Feilberg, A.: Negligible influence of livestock contaminants and sampling system on ammonia measurements with cavity ring-down spectroscopy, *Atmos. Meas. Tech.*, 12(5), 2837–2850, 2019.

Kim, H., Zhang, Q. and Heo, J.: Influence of intense secondary aerosol formation and long-range transport on aerosol chemistry and properties in the Seoul Metropolitan Area during spring time: results from KORUS-AQ, *Atmos. Chem. Phys.*, 18(10), 7149–7168, 2018.

Kim, P. S., Jacob, D. J., Fisher, J. A., Travis, K., Yu, K., Zhu, L., Yantosca, R. M., Sulprizio, M. P., Jimenez, J. L., Campuzano-Jost, P., Froyd, K. D., Liao, J., Hair, J. W., Fenn, M. A., Butler, C. F., Wagner, N. L., Gordon, T. D., Welti, A., Wennberg, P. O., Crounse, J. D., St Clair, J. M., Teng, A. P., Millet, D. B., Schwarz, J. P., Markovic, M. Z. and Perring, A. E.: Sources, seasonality, and trends of southeast US aerosol: an integrated analysis of surface, aircraft, and satellite observations with the GEOS-Chem chemical transport model, *Atmos. Chem. Phys.*, 15, 10411–10433, 2015.

Kline, J., Huebert, B., Howell, S., Blomquist, B., Zhuang, J., Bertram, T. and Carrillo, J.: Aerosol composition and size versus altitude measured from the C-130 during ACE-Asia, *J. Geophys. Res.*, 109(D19), 340, 2004.

Klockow, D., Jablonski, B. and Nießner, R.: Possible artifacts in filter sampling of atmospheric sulphuric acid and acidic sulphates, *Atmos. Environ.*, 13(12), 1665–1676, 1979.

Koutrakis, P., Wolfson, J. M. and Spengler, J. D.: An improved method for measuring aerosol strong acidity: Results from a nine-month study in St Louis, Missouri and Kingston, Tennessee, *Atmos. Environ.*, 22(1), 157–162, 1988.

Kupc, A., Williamson, C., Wagner, N. L., Richardson, M. and Brock, C. A.: Modification, calibration, and performance of the Ultra-High Sensitivity Aerosol Spectrometer for particle size distribution and volatility measurements during the Atmospheric Tomography Mission (ATom)

airborne campaign, *Atmos. Meas. Tech.*, 11(1), 369–383, 2018.

Larson, T. V., Covert, D. S., Frank, R. and Charlson, R. J.: Ammonia in the human airways: neutralization of inspired acid sulfate aerosols, *Science*, 197(4299), 161–163, 1977.

Lavery, T. F., Rogers, C. M., Baumgardner, R. and Mishoe, K. P.: Intercomparison of Clean Air Status and Trends Network Nitrate and Nitric Acid Measurements with Data from Other Monitoring Programs, *J. Air Waste Manag. Assoc.*, 59(2), 214–226, 2009.

Liao, J., Froyd, K. D., Murphy, D. M., Keutsch, F. N., Yu, G., Wennberg, P. O., St Clair, J. M., Crouse, J. D., Wisthaler, A., Mikoviny, T., Jimenez, J. L., Campuzano-Jost, P., Day, D. A., Hu, W., Ryerson, T. B., Pollack, I. B., Peischl, J., Anderson, B. E., Ziemba, L. D., Blake, D. R., Meinardi, S. and Diskin, G.: Airborne measurements of organosulfates over the continental U.S., *J. Geophys. Res. D: Atmos.*, 120(7), 2990–3005, 2015.

Liggio, J., Li, S.-M., Vlasenko, A., Stroud, C. and Makar, P.: Depression of ammonia uptake to sulfuric acid aerosols by competing uptake of ambient organic gases, *Environ. Sci. Technol.*, 45(7), 2790–2796, 2011.

Li, M., Weschler, C. J., Bekö, G., Wargocki, P., Lucic, G. and Williams, J.: Human Ammonia Emission Rates under Various Indoor Environmental Conditions, *Environ. Sci. Technol.*, doi:10.1021/acs.est.0c00094, 2020.

Liu, C.-N., Lin, S.-F., Awasthi, A., Tsai, C.-J., Wu, Y.-C. and Chen, C.-F.: Sampling and conditioning artifacts of PM_{2.5} in filter-based samplers, *Atmos. Environ.*, 85, 48–53, 2014.

Liu, C.-N., Lin, S.-F., Tsai, C.-J., Wu, Y.-C. and Chen, C.-F.: Theoretical model for the evaporation loss of PM_{2.5} during filter sampling, *Atmos. Environ.*, 109, 79–86, 2015.

Liu, M., Huang, X., Song, Y., Tang, J., Cao, J., Zhang, X., Zhang, Q., Wang, S., Xu, T., Kang, L., Cai, X., Zhang, H., Yang, F., Wang, H., Yu, J. Z., Lau, A. K. H., He, L., Huang, X., Duan, L., Ding, A., Xue, L., Gao, J., Liu, B. and Zhu, T.: Ammonia emission control in China would mitigate haze pollution and nitrogen deposition, but worsen acid rain, *Proc. Natl. Acad. Sci. U. S. A.*, 116(16), 7760–7765, 2019.

Liu, T., Clegg, S. L. and Abbatt, J. P. D.: Fast oxidation of sulfur dioxide by hydrogen peroxide in deliquesced aerosol particles, *Proc. Natl. Acad. Sci. U. S. A.*, 117(3), 1354–1359, 2020.

Liu, X., Zhang, Y., Huey, L. G., Yokelson, R. J., Wang, Y., Jimenez, J. L., Campuzano-Jost, P., Beyersdorf, A. J., Blake, D. R., Choi, Y., St. Clair, J. M., Crouse, J. D., Day, D. A., Diskin, G. S., Fried, A., Hall, S. R., Hanisco, T. F., King, L. E., Meinardi, S., Mikoviny, T., Palm, B. B., Peischl, J., Perring, A. E., Pollack, I. B., Ryerson, T. B., Sachse, G., Schwarz, J. P., Simpson, I. J., Tanner, D. J., Thornhill, K. L., Ullmann, K., Weber, R. J., Wennberg, P. O., Wisthaler, A., Wolfe, G. M. and Ziemba, L. D.: Agricultural fires in the southeastern U.S. during SEAC⁴RS: Emissions of trace gases and particles and evolution of ozone, reactive nitrogen, and organic aerosol, *J. Geophys. Res. D: Atmos.*, 121(12), 7383–7414, 2016.

- Liu, X., Huey, L. G., Yokelson, R. J., Selimovic, V., Simpson, I. J., Müller, M., Jimenez, J. L., Campuzano-Jost, P., Beyersdorf, A. J., Blake, D. R., Butterfield, Z., Choi, Y., Crouse, J. D., Day, D. A., Diskin, G. S., Dubey, M. K., Fortner, E., Hanisco, T. F., Hu, W., King, L. E., Kleinman, L., Meinardi, S., Mikoviny, T., Onasch, T. B., Palm, B. B., Peischl, J., Pollack, I. B., Ryerson, T. B., Sachse, G. W., Sedlacek, A. J., Shilling, J. E., Springston, S., St. Clair, J. M., Tanner, D. J., Teng, A. P., Wennberg, P. O., Wisthaler, A. and Wolfe, G. M.: Airborne measurements of western U.S. wildfire emissions: Comparison with prescribed burning and air quality implications, *J. Geophys. Res. D: Atmos.*, 122(11), 6108–6129, 2017.
- Malm, W. C., Sisler, J. F., Huffman, D., Eldred, R. A. and Cahill, T. A.: Spatial and seasonal trends in particle concentration and optical extinction in the United States, *J. Geophys. Res.*, 99(D1), 1347, 1994.
- Malm, W. C., Schichtel, B. A., Hand, J. L. and Collett, J. L., Jr.: Concurrent Temporal and Spatial Trends in Sulfate and Organic Mass Concentrations Measured in the IMPROVE Monitoring Program, *J. Geophys. Res. D: Atmos.*, 122(19), 10,462–10,476, 2017.
- Martin, N. A., Ferracci, V., Cassidy, N. and Hoffnagle, J. A.: The application of a cavity ring-down spectrometer to measurements of ambient ammonia using traceable primary standard gas mixtures, *Appl. Phys. B*, 122(8), 219, 2016.
- Ma, S.-S., Yang, W., Zheng, C.-M., Pang, S.-F. and Zhang, Y.-H.: Subsecond measurements on aerosols: From hygroscopic growth factors to efflorescence kinetics, *Atmos. Environ.*, 210, 177–185, 2019.
- McNaughton, C. S., Clarke, A. D., Howell, S. G., Pinkerton, M., Anderson, B., Thornhill, L., Hudgins, C., Winstead, E., Dibb, J. E., Scheuer, E. and Maring, H.: Results from the DC-8 Inlet Characterization Experiment (DICE): Airborne versus surface sampling of mineral dust and sea salt aerosols, *Aerosol Sci. Technol.*, 41(2), 136–159, 2007.
- Meskhidze, N., Chameides, W. L., Nenes, A. and Chen, G.: Iron mobilization in mineral dust: Can anthropogenic SO₂ emissions affect ocean productivity?, *Geophys. Res. Lett.*, 30(21), 2085, 2003.
- Mezuman, K., Bauer, S. E. and Tsigaridis, K.: Evaluating secondary inorganic aerosols in three dimensions, *Atmos. Chem. Phys.*, 16(16), 10651–10669, 2016.
- Middlebrook, A. M., Bahreini, R., Jimenez, J. L. and Canagaratna, M. R.: Evaluation of Composition-Dependent Collection Efficiencies for the Aerodyne Aerosol Mass Spectrometer using Field Data, *Aerosol Sci. Technol.*, 46(3), 258–271, 2012.
- Müller, M., Mikoviny, T., Feil, S., Haidacher, S., Hanel, G., Hartungen, E., Jordan, A., Märk, L., Mutschlechner, P., Schottkowsky, R., Sulzer, P., Crawford, J. H. and Wisthaler, A.: A compact PTR-ToF-MS instrument for airborne measurements of volatile organic compounds at high spatiotemporal resolution, , doi:10.5194/amt-7-3763-2014, 2014.
- Murphy, D. M. and Thomson, D. S.: Laser Ionization Mass Spectroscopy of Single Aerosol

Particles, *Aerosol Sci. Technol.*, 22(3), 237–249, 1995.

Murphy, D. M., Froyd, K. D., Schwarz, J. P. and Wilson, J. C.: Observations of the chemical composition of stratospheric aerosol particles: The Composition of Stratospheric Particles, *Q.J.R. Meteorol. Soc.*, 140(681), 1269–1278, 2014.

Murray, B. J. and Bertram, A. K.: Inhibition of solute crystallisation in aqueous $\text{H}^+ - \text{NH}_4^+ - \text{SO}_4^{2-} - \text{H}_2\text{O}$ droplets, *Phys. Chem. Chem. Phys.*, 10(22), 3287, 2008.

Myhre, G., Shindell, D., Bréon, F.-M., Collins, W., Fuglestedt, J., Huang, J., Koch, D., Lamarque, J.-F., Lee, D., Mendoza, B., Nakajima, T., Robock, A., Stephens, G., Takemura, T. and Zhang, H.: Anthropogenic and Natural Radiative Forcing, in *Climate Change 2013: The Physical Science Basis. Contribution of Working Group I to the Fifth Assessment Report of the Intergovernmental Panel on Climate Change*, edited by T. F. Stocker, D. Qin, G.-K. Plattner, M. Tignor, S. K. Allen, J. Boschung, A. Nauels, Y. Xia, V. Bex, and P. M. Midgley, p. 659, Cambridge University Press, Cambridge, United Kingdom and New York, NY, USA., 2013.

National Research Council: *The Airliner Cabin Environment and the Health of Passengers and Crew*, The National Academies Press, Washington, DC., 2002.

Nault, B. A., Campuzano-Jost, P., Day, D. A., Schroder, J. C., Anderson, B., Beyersdorf, A. J., Blake, D. R., Brune, W. H., Choi, Y., Corr, C. A., de Gouw, J. A., Dibb, J., DiGangi, J. P., Diskin, G. S., Fried, A., Huey, L. G., Kim, M. J., Knute, C. J., Lamb, K. D., Lee, T., Park, T., Pusede, S. E., Scheuer, E., Thornhill, K. L., Woo, J.-H. and Jimenez, J. L.: Secondary Organic Aerosol Production from Local Emissions Dominates the Organic Aerosol Budget over Seoul, South Korea, during KORUS-AQ, *Atmos. Chem. Phys.*, 18, 17769–17800, 2018.

Nenes, A., Pandis, S. N., Kanakidou, M., Russell, A., Song, S., Vasilakos, P. and Weber, R. J.: Aerosol acidity and liquid water content regulate the dry deposition of inorganic reactive nitrogen, *Atmos. Phys. Chem. Discuss.*, doi:10.5194/acp-2020-266, 2020a.

Nenes, A., Pandis, S. N., Weber, R. J. and Russell, A.: Aerosol pH and liquid water content determine when particulate matter is sensitive to ammonia and nitrate availability, *Atmos. Chem. Phys.*, 20(5), 3249–3258, 2020b.

Nguyen, T. K. V., Zhang, Q., Jimenez, J. L., Pike, M. and Carlton, A. G.: Liquid water: Ubiquitous contributor to aerosol mass, *Environ. Sci. Technol. Lett.*, 3, 257–263, 2016.

Nie, W., Wang, T., Gao, X., Pathak, R. K., Wang, X., Gao, R., Zhang, Q., Yang, L. and Wang, W.: Comparison among filter-based, impactor-based and continuous techniques for measuring atmospheric fine sulfate and nitrate, *Atmos. Environ.*, 44(35), 4396–4403, 2010.

Pagonis, D., Price, D. J., Algrim, L. B., Day, D. A., Handschy, A. V., Stark, H., Miller, S. L., de Gouw, J., Jimenez, J. L. and Ziemann, P. J.: Time-Resolved Measurements of Indoor Chemical Emissions, Deposition, and Reactions in a University Art Museum, *Environ. Sci. Technol.*, 53(9), 4794–4802, 2019.

Paulot, F., Jacob, D. J., Johnson, M. T., Bell, T. G., Baker, A. R., Keene, W. C., Lima, I. D., Doney, S. C. and Stock, C. A.: Global oceanic emission of ammonia: Constraints from seawater and atmospheric observations, *Global Biogeochem. Cycles*, 29(8), 1165–1178, 2015.

Pratt, K. A. and Prather, K. A.: Aircraft measurements of vertical profiles of aerosol mixing states, *J. Geophys. Res.*, 115(D11), D11305, 2010.

Price, H. C., Mattsson, J., Zhang, Y., Bertram, A. K., Davies, J. F., Grayson, J. W., Martin, S. T., O’Sullivan, D., Reid, J. P., Rickards, A. M. J. and Murray, B. J.: Water diffusion in atmospherically relevant α -pinene secondary organic material, *Chem. Sci.*, 6(8), 4876–4883, 2015.

Pye, H. O. T., Nenes, A., Alexander, B., Ault, A. P., Barth, M. C., Clegg, S. L., Collett, J. L., Jr., Fahey, K. M., Hennigan, C. J., Herrmann, H., Kanakidou, M., Kelly, J. T., Ku, I.-T., McNeill, V. F., Riemer, N., Schaefer, T., Shi, G., Tilgner, A., Walker, J. T., Wang, T., Weber, R., Xing, J., Zaveri, R. A. and Zuend, A.: The Acidity of Atmospheric Particles and Clouds, *Atmos. Chem. Phys.*, 20(8), 4809–4888, 2020.

Robbins, R. C. and Cadle, R. D.: Kinetics of the Reaction between Gaseous Ammonia and Sulfuric Acid Droplets in an Aerosol, *J. Phys. Chem.*, 62(4), 469–471, 1958.

Rumble, J. R., Ed.: *CRC Handbook of Chemistry and Physics*, 100th Edition, 2019 - 2020, Taylor & Francis Group., 2019.

Schauer, C., Niessner, R. and Pöschl, U.: Polycyclic aromatic hydrocarbons in urban air particulate matter: decadal and seasonal trends, chemical degradation, and sampling artifacts, *Environ. Sci. Technol.*, 37(13), 2861–2868, 2003.

Schroder, J. C., Campuzano-Jost, P., Day, D. A., Shah, V., Larson, K., Sommers, J. M., Sullivan, A. P., Campos, T., Reeves, J. M., Hills, A., Hornbrook, R. S., Blake, N. J., Scheuer, E., Guo, H., Fibiger, D. L., McDuffie, E. E., Hayes, P. L., Weber, R. J., Dibb, J. E., Apel, E. C., Jaeglé, L., Brown, S. S., Thornton, J. A. and Jimenez, J. L.: Sources and Secondary Production of Organic Aerosols in the Northeastern US during WINTER, *J. Geophys. Res. D: Atmos.*, doi:10.1029/2018JD028475, 2018.

Seinfeld., J. H. and Pandis, S. N.: *Atmospheric Chemistry and Physics: From Air Pollution to Climate Change*, Second., John Wiley & Sons, Inc., Hoboken, NJ USA., 2006.

Shingler, T., Crosbie, E., Ortega, A., Shiraiwa, M., Zuend, A., Beyersdorf, A., Ziemba, L., Anderson, B., Thornhill, L., Perring, A. E., Schwarz, J. P., Campuzano-Jost, P., Day, D. A., Jimenez, J. L., Hair, J. W., Mikoviny, T., Wisthaler, A. and Sorooshian, A.: Airborne characterization of subsaturated aerosol hygroscopicity and dry refractive index from the surface to 6.5 km during the SEAC⁴ RS campaign, *J. Geophys. Res. D: Atmos.*, 121(8), 4188–4210, 2016.

Shiraiwa, M., Ammann, M., Koop, T. and Pöschl, U.: Gas uptake and chemical aging of

semisolid organic aerosol particles, *Proc. Natl. Acad. Sci. U. S. A.*, 108(27), 11003–11008, 2011.

Slade, J. H., Ault, A. P., Bui, A. T., Ditto, J. C., Lei, Z., Bondy, A. L., Olson, N. E., Cook, R. D., Desrochers, S. J., Harvey, R. M., Erickson, M. H., Wallace, H. W., Alvarez, S. L., Flynn, J. H., Boor, B. E., Petrucci, G. A., Gentner, D. R., Griffin, R. J. and Shepson, P. B.: Bouncer Particles at Night: Biogenic Secondary Organic Aerosol Chemistry and Sulfate Drive Diel Variations in the Aerosol Phase in a Mixed Forest, *Environ. Sci. Technol.*, 53(9), 4977–4987, 2019.

Solomon, P. A., Mitchell, W., Tolocka, M., Norris, G., Gemmill, D., Wiener, R., Vanderpool, R., Murdoch, R., Natarajan, S. and Hardison, E.: Evaluation of PM_{2.5} Chemical Speciation Samplers for Use in the EPA National PM_{2.5} Chemical Speciation Network, EPA., 2000.

Solomon, P. A., Crumpler, D., Flanagan, J. B., Jayanty, R. K. M., Rickman, E. E. and McDade, C. E.: U.S. national PM_{2.5} Chemical Speciation Monitoring Networks-CSN and IMPROVE: description of networks, *J. Air Waste Manag. Assoc.*, 64(12), 1410–1438, 2014.

Song, S., Gao, M., Xu, W., Shao, J., Shi, G., Wang, S., Wang, Y., Sun, Y. and McElroy, M. B.: Fine-particle pH for Beijing winter haze as inferred from different thermodynamic equilibrium models, *Atmos. Chem. Phys.*, 18(10), 7423–7438, 2018.

Spiller, L. L.: Determination of Ammonia/Air Diffusion Coefficient Using Nafion Lined Tube, *Anal. Lett.*, 22(11-12), 2561–2573, 1989.

Stith, J. L., Ramanathan, V., Cooper, W. A., Roberts, G. C., DeMott, P. J., Carmichael, G., Hatch, C. D., Adhikary, B., Twohy, C. H., Rogers, D. C., Baumgardner, D., Prenni, A. J., Campos, T., Gao, R., Anderson, J. and Feng, Y.: An overview of aircraft observations from the Pacific Dust Experiment campaign, *J. Geophys. Res.*, 114(D5), 833, 2009.

Sueper, D.: ToF-AMS Data Analysis Software Webpage, [online] Available from: http://cires1.colorado.edu/jimenez-group/wiki/index.php/ToF-AMS_Analysis_Software, 2018.

Sun, K., Cady-Pereira, K., Miller, D. J., Tao, L., Zondlo, M. A., Nowak, J. B., Neuman, J. A., Mikoviny, T., Müller, M., Wisthaler, A., Scarino, A. J. and Hostetler, C. A.: Validation of TES ammonia observations at the single pixel scale in the San Joaquin Valley during DISCOVER-AQ, *J. Geophys. Res. D: Atmos.*, 120(10), 5140–5154, 2015.

Sun, Y., Zhang, Q., Macdonald, A. M., Hayden, K., Li, S. M., Liggió, J., Liu, P. S. K., Anlauf, K. G., Leaitch, W. R., Steffen, A., Cubison, M., Worsnop, D. R., van Donkelaar, A. and Martin, R. V.: Size-resolved aerosol chemistry on Whistler Mountain, Canada with a high-resolution aerosol mass spectrometer during INTEX-B, *Atmos. Chem. Phys.*, 9(9), 3095–3111, 2009.

Sutton, M. A., Dragosits, U., Tang, Y. S. and Fowler, D.: Ammonia emissions from non-agricultural sources in the UK, *Atmos. Environ.*, 34(6), 855–869, 2000.

Sutton, M. A., Reis, S., Riddick, S. N., Dragosits, U., Nemitz, E., Theobald, M. R., Tang, Y. S., Braban, C. F., Vieno, M., Dore, A. J., Mitchell, R. F., Wanless, S., Daunt, F., Fowler, D., Blackall, T. D., Milford, C., Flechard, C. R., Loubet, B., Massad, R., Cellier, P., Personne, E.,

Coheur, P. F., Clarisse, L., Van Damme, M., Ngadi, Y., Clerbaux, C., Skjøth, C. A., Geels, C., Hertel, O., Wichink Kruit, R. J., Pinder, R. W., Bash, J. O., Walker, J. T., Simpson, D., Horváth, L., Misselbrook, T. H., Bleeker, A., Dentener, F. and de Vries, W.: Towards a climate-dependent paradigm of ammonia emission and deposition, *Philos. Trans. R. Soc. Lond. B Biol. Sci.*, 368(1621), 20130166, 2013.

Swartz, E., Shi, Q., Davidovits, P., Jayne, J. T., Worsnop, D. R. and Kolb, C. E.: Uptake of Gas-Phase Ammonia. 2. Uptake by Sulfuric Acid Surfaces, *J. Phys. Chem. A*, 103(44), 8824–8833, 1999.

Talbot, R. W., Dibb, J. E., Lefer, B. L., Scheuer, E. M., Bradshaw, J. D., Sandholm, S. T., Smyth, S., Blake, D. R., Blake, N. J., Sachse, G. W., Collins, J. E. and Gregory, G. L.: Large-scale distributions of tropospheric nitric, formic, and acetic acids over the western Pacific basin during wintertime, *J. Geophys. Res.: Atmos.*, 102(D23), 28303–28313, 1997.

Tao, Y. and Murphy, J. G.: The sensitivity of PM_{2.5} acidity to meteorological parameters and chemical composition changes: 10-year records from six Canadian monitoring sites, *Atmos. Chem. Phys.*, 19(14), 9309–9320, 2019.

Thomson, D. S., Schein, M. E. and Murphy, D. M.: Particle Analysis by Laser Mass Spectrometry WB-57F Instrument Overview, *Aerosol Sci. Technol.*, 33(1-2), 153–169, 2000.

Toon, O. B., Maring, H., Dibb, J., Ferrare, R., Jacob, D. J., Jensen, E. J., Luo, Z. J., Mace, G. G., Pan, L. L., Pfister, L., Rosenlof, K. H., Redemann, J., Reid, J. S., Singh, H. B., Thompson, A. M., Yokelson, R., Minnis, P., Chen, G., Jucks, K. W. and Pszenny, A.: Planning, implementation, and scientific goals of the Studies of Emissions and Atmospheric Composition, Clouds and Climate Coupling by Regional Surveys (SEAC⁴RS) field mission, *J. Geophys. Res. D: Atmos.*, 121(9), 4967–5009, 2016.

Vay, S. A., Woo, J.-H., Anderson, B. E., Thornhill, K. L., Blake, D. R., Westberg, D. J., Kiley, C. M., Avery, M. A., Sachse, G. W., Streets, D. G., Tsutsumi, Y. and Nolf, S. R.: Influence of regional-scale anthropogenic emissions on CO₂ distributions over the western North Pacific, *J. Geophys. Res.*, 108(D20), 213, 2003.

Vay, S. A., Choi, Y., Vadrevu, K. P., Blake, D. R., Tyler, S. C., Wisthaler, A., Hecobian, A., Kondo, Y., Diskin, G. S., Sachse, G. W., Woo, J.-H., Weinheimer, A. J., Burkhardt, J. F., Stohl, A. and Wennberg, P. O.: Patterns of CO₂ and radiocarbon across high northern latitudes during International Polar Year 2008, *J. Geophys. Res.*, 116(D14), 4039, 2011.

Walker, J. M., Philip, S., Martin, R. V. and Seinfeld, J. H.: Simulation of nitrate, sulfate, and ammonium aerosols over the United States, *Atmos. Chem. Phys.*, 12(22), 11213–11227, 2012.

Wang, J., Hoffmann, A. A., Park, R. J., Jacob, D. J. and Martin, S. T.: Global distribution of solid and aqueous sulfate aerosols: Effect of the hysteresis of particle phase transitions, *J. Geophys. Res.*, 113(D11), 1770, 2008a.

Wang, J., Jacob, D. J. and Martin, S. T.: Sensitivity of sulfate direct climate forcing to the

hysteresis of particle phase transitions, *J. Geophys. Res.*, 113(D11), 13791, 2008b.

Warneke, C., Schwarz, J. P., Ryerson, T., Crawford, J., Dibb, J., Lefer, B., Roberts, J., Trainer, M., Murphy, D., Brown, S., Brewer, A., Gao, R.-S. and Fahey, D.: Fire Influence on Regional to Global Environments and Air Quality (FIREX-AQ): A NOAA/NASA Interagency Intensive Study of North American Fires, NOAA/NASA. [online] Available from: <https://esrl.noaa.gov/csd/projects/firex-aq/whitepaper.pdf>, 2018.

Warner, J. X., Wei, Z., Larrabee Strow, L., Dickerson, R. R. and Nowak, J. B.: The global tropospheric ammonia distribution as seen in the 13-year AIRS measurement record, *Atmos. Chem. Phys.*, 16(8), 5467–5479, 2016.

Warner, J. X., Dickerson, R. R., Wei, Z., Strow, L. L., Wang, Y. and Liang, Q.: Increased atmospheric ammonia over the world's major agricultural areas detected from space, *Geophys. Res. Lett.*, 44(6), 2875–2884, 2017.

Watson, J. G., Chow, J. C., Chen, L. W. A. and Frank, N. H.: Methods to assess carbonaceous aerosol sampling artifacts for IMPROVE and other long-term networks, *J. Air Waste Manag. Assoc.*, 59(8), 898–911, 2009.

Weber, R. J., Orsini, D., Daun, Y., Lee, Y.-N., Klotz, P. J. and Brechtel, F.: A Particle-into-Liquid Collector for Rapid Measurement of Aerosol Bulk Chemical Composition, *Aerosol Sci. Technol.*, 35(3), 718–727, 2001.

Weber, R. J., Guo, H., Russell, A. G. and Nenes, A.: High aerosol acidity despite declining atmospheric sulfate concentrations over the past 15 years, *Nat. Geosci.*, 9(4), 282–285, 2016.

Williamson, C., Kupc, A., Wilson, J., Gesler, D. W., Reeves, J. M., Erdesz, F., McLaughlin, R. and Brock, C. A.: Fast time response measurements of particle size distributions in the 3–60 nm size range with the nucleation mode aerosol size spectrometer, *Atmos. Meas. Tech.*, 11(6), 3491–3509, 2018.

Wilson, R. E.: Humidity Control by Means of Sulfuric Acid Solutions, with Critical Compilation of Vapor Pressure Data, *J. Ind. Eng. Chem.*, 13(4), 326–331, 1921.

Worsnop, D. R., Williams, L. R., Kolb, C. E., Mozurkewich, M., Gershenson, M. and Davidovits, P.: Comment on “The NH_3 Mass Accommodation Coefficient for Uptake onto Sulfuric Acid Solution,” *J. Phys. Chem. A*, 108(40), 8546–8548, 2004.

Yao, X. H. and Zhang, L.: Supermicron modes of ammonium ions related to fog in rural atmosphere, *Atmos. Chem. Phys.*, 12(22), 11165–11178, 2012.

Zakoura, M., Kakavas, S., Nenes, A. and Pandis, S. N.: Size-resolved aerosol pH over Europe during summer, *Atmos. Chem. Phys. Discuss.*, doi:10.5194/acp-2019-1146, 2020.

Zhang, X., Smith, K. A., Worsnop, D. R., Jimenez, J., Jayne, J. T. and Kolb, C. E.: A Numerical Characterization of Particle Beam Collimation by an Aerodynamic Lens-Nozzle System: Part I.

An Individual Lens or Nozzle, *Aerosol Sci. Technol.*, 36(5), 617–631, 2002.

Zhang, X., Smith, K. A., Worsnop, D. R., Jimenez, J. L., Jayne, J. T., Kolb, C. E., Morris, J. and Davidovits, P.: Numerical Characterization of Particle Beam Collimation: Part II Integrated Aerodynamic-Lens–Nozzle System, *Aerosol Sci. Technol.*, 38(6), 619–638, 2004.

Zhou, S., Collier, S., Jaffe, D. A. and Zhang, Q.: Free tropospheric aerosols at the Mt. Bachelor Observatory: more oxidized and higher sulfate content compared to boundary layer aerosols, *Atmos. Chem. Phys.*, 19(3), 1571–1585, 2019.